

---

## **9. FOCUSED ION BEAM SYSTEM—A MULTIFUNCTIONAL TOOL FOR NANOTECHNOLOGY**

NAN YAO

### **I. INTRODUCTION**

With nanotechnology being at the forefront of modern day research and development, new knowledge and successful application of increasingly small technologies is in high demand. Having this in mind, it is clear that the advancement and production of new high grade tools is a necessity if we are to see industrial progress. In particular materials science, with its never ending push for smaller scale analysis, is constantly looking for new tools that will help characterize materials and phenomena in addition to being able to machine at micro and nano-scales.

One tool which is expected to continue having success in answering this plea is the focused ion beam (FIB). The machine is relatively new, with great potential in nanotechnology and material science, and so naturally, there is much interest in exploring its applications. It allows slim or even no disruption of a procedure in addition to having tremendous micro and nano-machining capabilities. This interest has resulted in the development of the two-beam FIB system, which has advanced hand in hand with the complexity of new materials. Materials now being developed have more geometric intricacies and smaller feature size than ever before. Such complexity is inherent in most biomaterials and their synthetic analogues, as well as in nanotechnology. Beyond the structural complexity, phenomena occurring on even smaller length scales often adversely affect the performance and reliability of these materials. Foremost among these is inter-diffusion among the layers, resulting in chemical and structural gradients (figure 1). Understanding and improving on the performance and durability of these

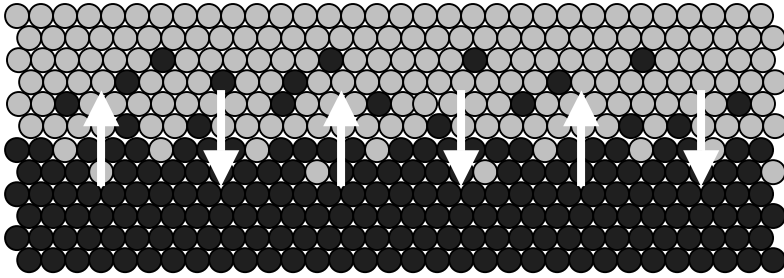


**Figure 1.** Schematic diagram of interlayer diffusion.

systems requires high-resolution structural, chemical and geometric analysis of cross sections through the layers, a function which the two-beam FIB system excels at.

This chapter is intended as a review of the major literature on the two-beam system. Since the FIB is an essential component of the two-beam, a survey of the FIB is presented first, followed by a discussion of the new or improved features of the two-beam system achieved by importing the scanning electron microscope (SEM). The goal is to discuss the wide spectrum of possibilities resulting from FIB technology, so as to serve as a reference guide for future work.

We begin by describing the fundamental differences between ions and electrons, and then continue to explain how these properties affect the structure and functionality of the FIB and SEM. After a brief explanation of the properties of interest and theory behind the FIB, we discuss various techniques for which it is most useful. Milling, of course, is a natural result of using relatively heavy ions in the beam. It allows precise modification of sample surfaces, as well as creating well defined cross-sections. The milling machine can easily be converted to a deposition system by using a gas delivery device to apply the desired chemical compound near the surface impact point of the ion beam. In conjunction with its milling potential, the FIB's deposition capabilities allow the creation of almost any micro-structure (figure 2). In addition, ion implantation, another technique available in the FIB system, is very useful in modifying certain materials. Of course, we also study the imaging possibilities of the FIB, where the large size of the ions can also provide advantages found in no other imaging tool. Once we've covered these aspects of the FIB, we discuss how these and other processes are improved by incorporating both the FIB and SEM into a single machine, justly named the two-beam FIB system. We will observe that in combining the two, we obtain capabilities that exceed anything found in either the FIB or SEM.

After discussing the advantages available from using the two-beam FIB system, we focus on several major areas of FIB applicability, beginning with its vast milling capabilities for surface modification of materials. Since the FIB machine is first and foremost a micro scale milling machine, its applications for material alteration are countless. We look into the ever advancing field of integrated circuits and discuss how the FIB can be used for defect analysis as well as structure modification. We also consider

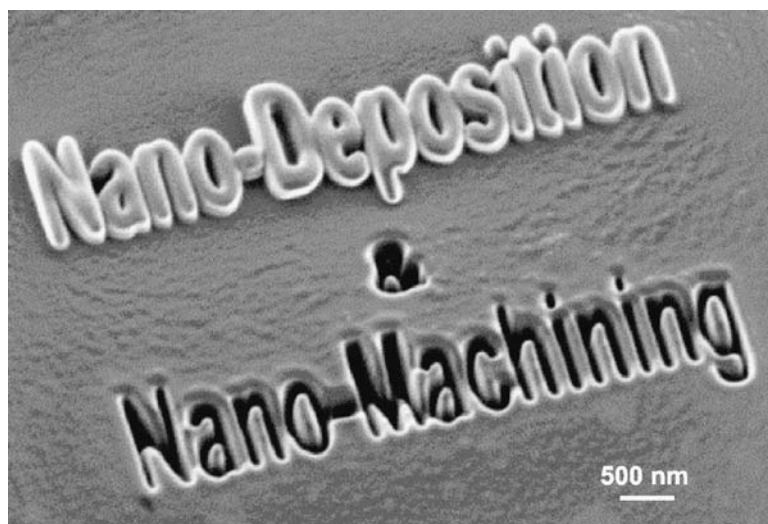


**Figure 2.** Example of the FIB's milling and deposition capabilities. (Courtesy of Fibics Incorporated)

the lithographic advantages of the FIB in addition to its brute physical capabilities of cross sectioning and sharpening, and proceed to study the characterization of the interaction between certain materials and focused ions.

In addition to milling, TEM sample preparation has been a widely studied and familiar use for the FIB machine, and thus is worth noting. The FIB can perform this function significantly faster than old methods, saving valuable time. For electron transparent samples, the FIB machine is able to thin out a region of a bulk material by digging trenches and subsequent shavings to make the samples as thin as possible. We discuss the basic techniques of lift-out and micro-pillar sampling, issues such as warping, and an environmental application of the FIB pertaining to TEM sample preparation.

We also take a deep look into the many imaging applications of the FIB in the two-beam system. Images can be obtained from a secondary electron detector using either the SEM or the FIB by simply toggling between the two. Each has its advantages depending on the specific needs. For example, using electrons to image, as in the SEM, entails much less damage to the material, while providing a much better resolution. On the other hand, ion beam imaging, found in the FIB, provides better sensitivity to details such as crystal orientations and grain structure because of the depth of penetration from channeling. The two-beam system is then an exceptionally practical machine, as it combines the crisp non destructive images of the scanning electron microscope with the milling capabilities of the focused ion beam. Additionally, we explore a very useful method of obtaining three-dimensional data by shaving off thin layers, and as a result, obtaining a series of two dimensional. With this data, available only from the combining SEM and FIB applications, graphs and images can easily be

interpolated with the two dimensional data. By then performing a secondary ion mass spectrometry (SIMS) analysis to yield elemental composition, we can have a complete set of data.

Finally, we comment on the sample damage that using the FIB can induce. Although this can sometimes be a problem, we will discuss ways of using this as an advantage. Even with this limiting quality, the FIB has tremendous breadth in its applicability, and deserves all the attention it has received as an important new technology.

## II. PRINCIPLES AND PRACTICE OF THE FOCUSED ION BEAM SYSTEM

A focused ion beam system is an effective combination of a scanning ion microscope and a precision machining tool. The FIB was developed as a result of research by Krohn in 1961 on liquid-metal ion sources (LMIS) for use in space [1]. Interested in developing thrusters that used charged metal droplets, he first documented ion emission from a liquid metal source [2]. The discovery of LMIS found novel applications in the areas of semiconductors and materials science. Commercialization of the FIB was occurred in the 1980's, mainly geared towards the growing semiconductor industry, but also finding a niche in the materials sciences industry.

The modern focused ion beam system utilizes a LMIS at the top of its column to produce ions, usually  $\text{Ga}^+$ . From here the ions are pulled out and focused into a beam by an electric field and subsequently passed through apertures, then scanned over the sample surface (figure 3). Upon impact, the ion-atom collision is either elastic or inelastic in nature. Elastic collisions result in the excavation of surface atoms—a term called sputtering—and are the primary cause of the actual modification of the material surface (figure 4). Inelastic collisions occur when the ions transfer some of their energy to either the surface atoms or electrons. This process produces secondary electrons (electrons which become excited and are able to escape from their shell), along with X rays (the energy released when an electron drops down into a lower shell). Secondary ions are also produced through the collision, seemingly after secondary electrons have been emitted.

Valuable information can be gathered from all emission, depending on the capabilities of the machine. The signals from the ejected ions, once collected, can be amplified and displayed to show the detailed structure of the sample surface. Beyond its imaging capabilities, the FIB can be used as a deposition tool by injecting an organometallic gas in the path of the ion beam, just above the sample surface. This technique proves to be practical for certain material repair applications. In addition, by containing the ion beam over a specific region of the sample for an extended length of time, the continuous sputtering process will lead to noticeable removal of material, which is useful for probing and milling applications.

The underlying factor in the physics behind the FIB is the fact that ions are significantly more massive than electrons (table 1), a remarkably enhancing feature. The collisions between the large primary ions and the substrate atoms cause surface alterations at various levels depending on dosage, overlap, dwell time, and many other variables, in a way that electrons cannot achieve [3].

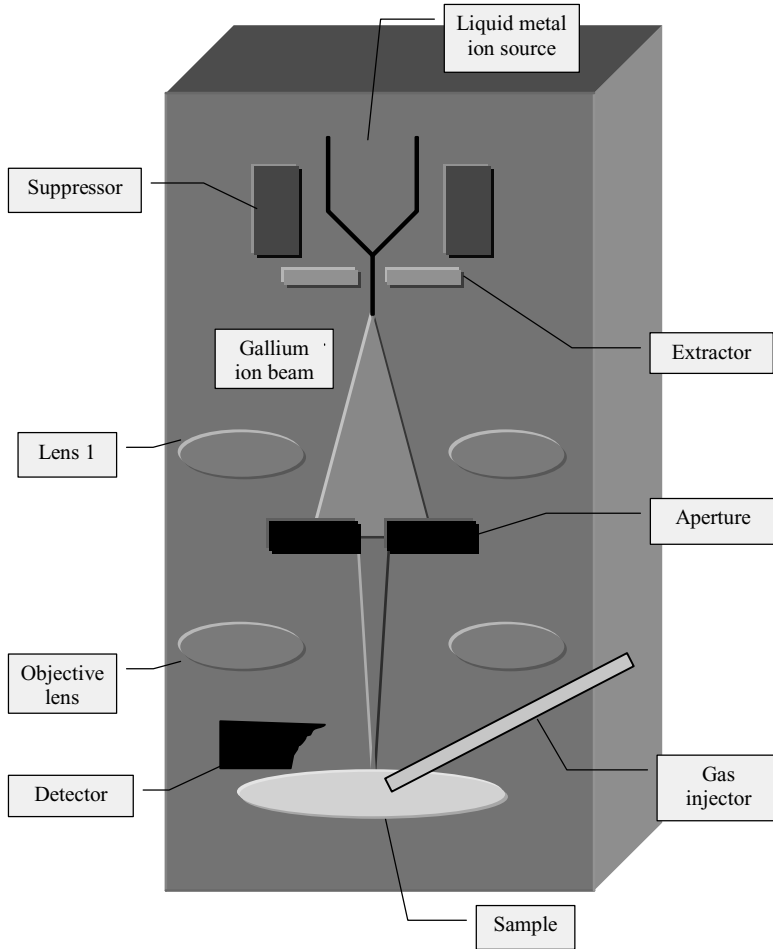


**Figure 3.** Schematic diagram of the FIB system.

The properties of the FIB system give it a unique ability to isolate a specific region of the sample, so as to only make necessary modifications without undermining the integrity of the entire sample. This has a wide range of applicability, from simple techniques like making probe holes to more complicated techniques such as cutting a precise three-dimensional cross-section of a sample. In addition, the FIB, having both drilling and deposition capabilities, is ideal for failure analysis and repair.

### 2.1. Ion Beam Versus Electron Beam

Because of the analogous nature of ion beam and electron beam microscopy, a comparison of the two can help provide a better understanding of the subject. The fundamental

**Table 1.** Quantitative Comparison of FIB Ions and SEM Electrons.

Particle:	FIB	SEM	Ratio
Type	Ga <sup>+</sup> ion	Electron	
Elementary charge	+1	-1	
Particle size	0.2 nm	0.00001 nm	20,000
Mass	$1.2 \times 10^{-25}$ kg	$9.1 \times 10^{-31}$ kg	130,000
Velocity at 30 kV	$2.8 \times 10^5$ m/s	$1.0 \times 10^8$ m/s	0.0028
Velocity at 2 kV	$7.3 \times 10^4$ m/s	$2.6 \times 10^7$ m/s	0.0028
Velocity at 1 kV	$5.2 \times 10^4$ m/s	$1.8 \times 10^7$ m/s	0.0028
Momentum at 30 kV	$3.4 \times 10^{-20}$ kgm/s	$9.1 \times 10^{-23}$ kgms	370
Momentum at 2 kV	$8.8 \times 10^{-21}$ kgm/s	$2.4 \times 10^{-23}$ kgm/s	370
Momentum at 1 kV	$6.2 \times 10^{-21}$ kgm/s	$1.6 \times 10^{-23}$ kgm/s	370
<i>Beam:</i>			
Size	nm range	nm range	
Energy	up to 30 kV	up to 30 kV	~
Current	pA to nA range	pA to $\mu$ A range	~
<i>Penetration depth:</i>			
In polymer at 30 kV	60 nm	12000 nm	0.005
In polymer at 2kV	12 nm	100 nm	0.12
In iron at 30 kV	20 nm	1800 nm	0.11
In iron at 2 kV	4 nm	25 nm	0.16
<i>Average signal per 100 particles at 20 kV:</i>			
Secondary electrons	100-200	50-75	
Back-scattered electron	0	30-50	0
Substrate atom	500	0	infinite
Secondary ion	30	0	infinite
X-ray	0	0.7	0

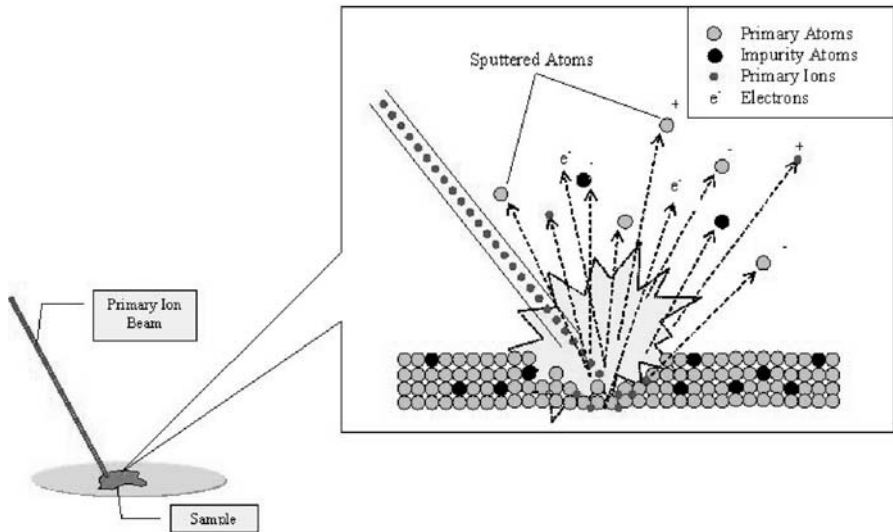


**Figure 4.** Schematic diagram of the ion beam sputtering process.

difference between these two techniques lies in the use of different charged particles for the primary incident beam; as their names suggest, the former utilizes ions while the latter relies on electrons. Ions and electrons have three major differences. To begin with, electrons are negatively charged while ions can be positively charged. This alone does not have any significant consequence, but the other two differences—size and mass—can appreciably alter the interactions between the beam and the sample. These differences are shown quantitatively in table 1.

When a beam of energetic particles, be it ions or electrons, strikes a solid surface, several processes get underway in the area of interaction. A fraction of the particles are backscattered from the surface layers, while the others are slowed down within the solid. Unlike electrons though, the relatively large ions have a difficult time penetrating the sample by passing between individual atoms. Their size increases the probability of interaction with atoms, causing a rapid loss of energy. As a result, ion-atom interaction mainly involves the outer shell, resulting in atomic ionization and breaking of the chemical bonds of the surface atoms. This is the source of secondary electrons and the cause of changes in the chemical state of the material. Similarly, since the inner electrons of the sample cannot be reached by the incoming ion beam, inner shell excitation does not occur, and as a result, usable X-rays are not likely to be generated as is the case when using an electron beam.

The total length the ion travels is known as its “penetration depth,” a term which also applies to electrons, although they often pass much deeper into the sample (table 1). The atomic collision has a statistical nature, and therefore, the penetration depth adheres to a symmetric Gaussian distribution around the mean value. The moving ion recoils one of the atoms in the sample, which then causes another constituent atom to recoil. As a result, the ions create many atomic defects along their path. This generation of defects plays an important role when using an ion beam for material modifications.

As for the difference in mass, ions—being many times heavier—can carry about 370 times the momentum of electrons. Upon contact, this momentum can be transferred to the atoms in the sample, causing enough motion to remove the atoms from their aligned positions. This sputtering effect, not present when an electron beam is used, has important milling applications which are discussed later. The key idea to remember is that as a result of the ions’ large size and mass, an ion beam surpasses the functional range of an electron beam by removing atoms from the sample surface in a precise, controlled manner.

In particular, gallium ( $\text{Ga}^+$ ) ions are used in the FIB for several reasons. Firstly, its low melting point makes gallium convenient in that it requires only limited heating, and therefore is in the liquid phase during operation. Also, its mass is just about ideal, as it is heavy enough to allow milling of the heavier elements, but not so heavy that it will destroy a sample immediately. Finally, since some of the ions used in the beam will be implanted into the sample, it is important to use an element that will not interfere with the analysis of the sample. Gallium can easily be distinguished from other elements, and therefore does not cause trouble in this regard. Although gallium is not the only possible choice, it has become the popular ion for use in the FIB system.

Unlike with electrons, the collision using a gallium ion beam induces secondary processes such as recoil and sputtering of constituent atoms, defect formation, electron excitation and emission, and photon emission. Thermal and radiation-induced diffusion contribute to various phenomena of interdiffusion of constituent elements, phase transformation, amorphization, crystallization, track formation, permanent damage, and so on. Ion implantation and sputtering change the surface morphology; craters, facets, grooves, ridges, pyramids, blistering, exfoliation, and a spongy surface may develop. All of these are interrelated in a complicated way, so that a single phenomenon cannot be understood without discussing several of these processes. Therefore, it is necessary to quantitatively understand the experimental observations and to have stringent design abilities for sophisticated applications of these versatile processes in the field of nanotechnology. With that, we can aim at material modification, deposition, implantation, erosion, nanofabrication, surface analysis, and a seemingly endless list of other applications.

## 2.2. Focused Ion Beam Microscope Versus Scanning Electron Microscope

The differences between ions and electrons can be extended to their respective machines, the FIB system and the scanning electron microscope (SEM). The two are designed and work very similarly, but the FIB's use of gallium ions from a field emission liquid metal ion (FE-LMI) source rather than electrons provides functionality and applicability different from that of the SEM. As discussed in the previous section, this focused primary beam of gallium ions is rastered on the surface of the material to be analyzed. As it hits the surface, a small amount of material is sputtered, or dislodged, from the surface. The dislodged material may be in the form of secondary ions, atoms, and secondary electrons. These are then collected and analyzed as signals to form an image on a screen as the primary beam scans the surface. This image forming capability allows high magnification microscopy in the FIB system.

In both the FIB and SEM machines, a source emits charged particles which are then focused into a beam and scanned across small areas of the sample using deflection plates or scan coils. In the SEM, the focusing is accomplished using magnetic lenses. Ions though, are much heavier and therefore slower than electrons, so the corresponding Lorenz force is lower. As a result, magnetic lenses are less effective on ions, so the FIB system is equipped with electrostatic lenses which prove much more effective in focusing the ions into a beam (figure 5).

Both instruments are used for high resolution imaging by collecting the secondary electrons produced by the beam's interaction with the sample surface. Contrast is formed by the fact that raised areas of the sample (hills) produce more collectable secondary electrons than depressed areas (valleys). A viewing monitor is synched to the scan coils controlling the beam so that as the beam scans across the sample surface, its image is reproduced on the screen. For the FIB, imaging resolution below 10 nm is possible. This image will show both topographic information and materials contrast and often provides information complementary to that obtained from an SEM image. Since the ion-solid interaction also depends on the crystal grain orientation,



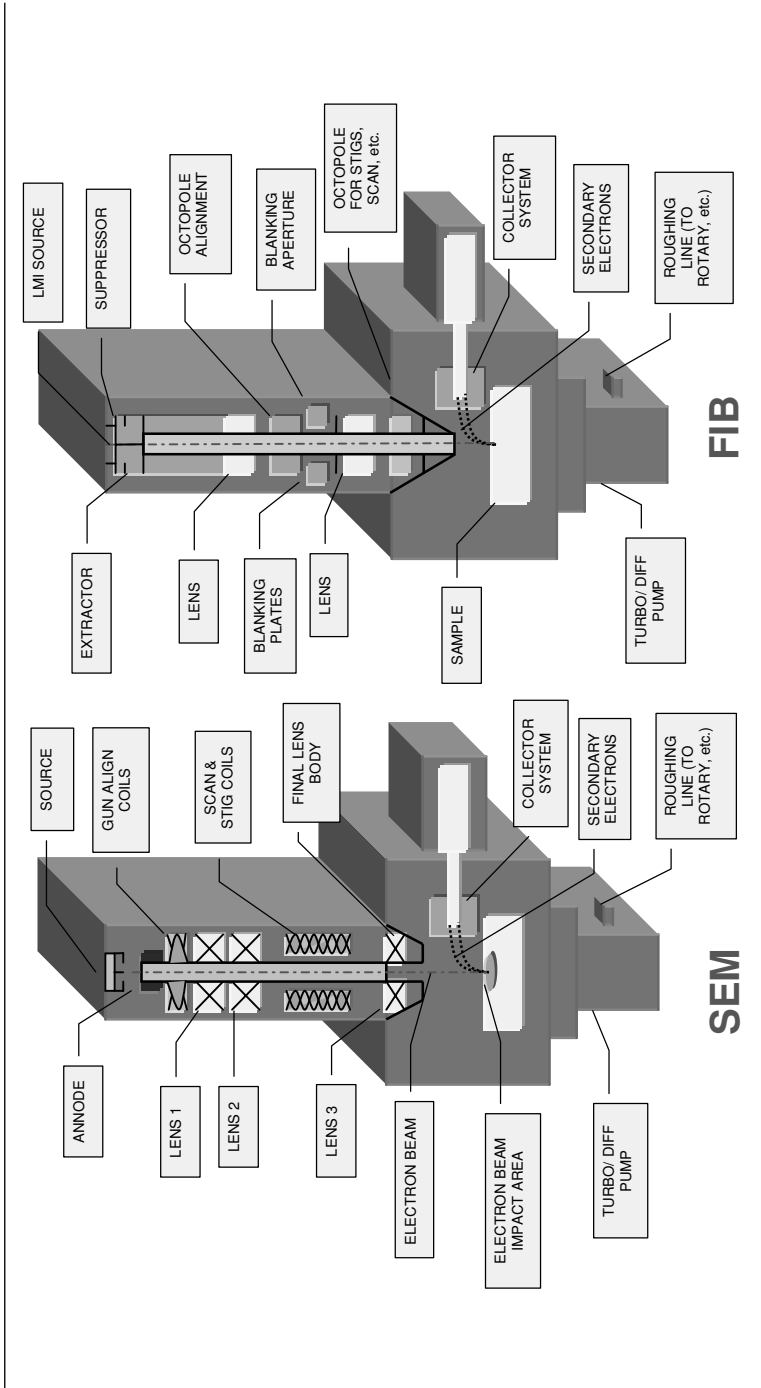


**Figure 5.** Schematic comparison of the SEM and FIB machines.

information concerning grain size and orientation can be obtained simply by collecting an image of the surface using the FIB. Note that although ions move much slower than electrons of the same energy, they are still fast compared to the image collection mode; in practice this has only negligible consequences, taking into account an image shift of a few pixels.

As for the sample itself, the FIB can accommodate wafer samples up to 8 inches (200 mm) in diameter; there is no minimum sample size. The sample must be vacuum compatible and conductive samples are preferred. Both individual and packaged parts can be used. Unlike in the SEM though, the sample will be altered during examination under the FIB, as the large, heavy ions will cause sputtering on the sample surface. Also, when using ions the sample often develops a positive charge which can distort the image. To combat this effect, an electron flood gun is used in the FIB to keep the sample more neutral.

### 2.3. Milling

By far the most powerful and versatile capability of the FIB system is milling. It adds a third dimension to microscopy, allowing us to modify the material surface, create cross sections, and carve materials into any shape we desire. For example, this method can provide electron-transparent, site-specific cross-sections of heterogeneous catalysts (figure 6). Again, when the relatively heavy and high-momentum ions collide with atoms on the sample surface, significant amounts of energy are transferred to the atoms, causing them to break bonds and leave their place in the atom matrix. Unlike electrons, which are hardly heavy enough to cause any atom movement in the sample (like trying to move a soccer ball by throwing ping pong balls at it), the ions, acting like soccer balls themselves, easily disrupt the placement and alignment of the atoms and create a sputtering effect. So when using an ion beam to bombard a sample, milling is a natural and continuous consequence. By controlling aspects the sputtering such as rate, location, and depth, we can take advantage of the FIB system's remarkable milling abilities.

In general, the higher the primary beam current, the faster material is sputtered from the surface. Therefore, if only high-magnification imaging is desired, a low-current beam must be used. For milling applications though, high-current beam operation is used to sputter or remove material from the surface initially, then a lower beam current is used for fine polishing. The sputtering rate can be easily and accurately controlled by altering the beam current or using smaller spot sizes. In addition, material sputter rate selectivity can be achieved through a process known as gas assisted etching (GAE). In this technique, one of several halogen gases is introduced to the work surface in the immediate vicinity of the desired hole or cut. The material-specific absorbcency rates enhance the formation of volatile products under ion bombardment. This allows oxides to be cleared without damage to conductors, and conductors to be cut without damage to underlying insulators. Typical resolution for cutting is around 0.1  $\mu\text{m}$ . The holes and cuts can be very accurately placed (usually within 20 nm) [4] and can reach buried layers provided that the depth to width aspect ratio is kept below 4:1. GAE,

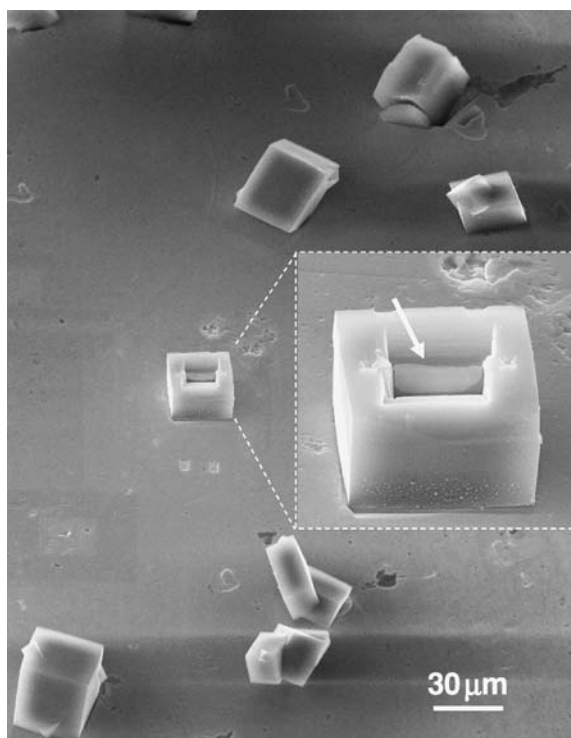


**Figure 6.** FIB sections from a heterogeneous catalyst. Arrow shows a thin sample slice that can be extracted from an individual small crystal.

often using iodine or xenon difluoride, can increase the aspect ratio to 8:1 or better. As a result, the milling efficiency is typically a few  $\mu\text{m}^3/\text{nC}$  but varies in different materials. The actual rate depends on the mass of the target atom, its binding energy to the atom matrix, and its matrix orientation with respect to the incident direction of the ion beam.

The GAE technique is more efficient in removing large volumes of material that would be prohibitively time-consuming otherwise. It is important to keep in mind that GAE is quite chemistry-specific, which gives us the ability to selectively etch one material without affecting the others. For example, materials like Si, Al and GaAs can have their removal rate increase 20 to 30 times through GAE, while oxides like  $\text{SiO}_2$  and  $\text{Al}_2\text{O}_3$  are not affected [5]. Similarly, in the presence of water vapor, carbon based materials show a highly enhanced removal rate whereas materials that oxidize, such as Al metallization lines and silicon, will actually show dramatically reduced rates [6].

In addition to changing the rate of material removal, GAE can be “neater” than ordinary ion milling, as redeposition of etched materials does not occur when using the former. However, the GAE technique has its problems as well. It contaminates

the sample deeper into the surface than simple ion milling [7]. Also, GAE does not have the pinpoint precision that ion milling can achieve. Oftentimes, a combination of initial GAE followed by ion milling is used when an operation requires bulk volumes of material removal as well as high precision.

With the FIB system, we have both lateral and depth control over the beam. Of course, if the beam is held over one area for a length of time, more material will be removed from that area. This process can be used to expose buried lines for eventual cutting or attaching to other circuit elements, depending on the desired modification of the structure. Unfortunately, an ion beam will not etch through unlimited thicknesses of material. By injecting a reactive gas into the mill process, the aspect ratio of the ion beam's cutting depth can be dramatically altered, depending on such variables as sample composition, mill area, beam parameters, and whether an enhanced etch process is used; this allows us to reach lower levels in the sample disturbing the upper layer. Having this precision and control allows applications unique to the FIB system.

#### 2.4. Deposition

The FIB demonstrates its versatility by how easily it can be converted from a micro-milling system to a deposition system. A simple adjustment allows the addition of material instead of the usual sputtering and removal of material. To create this change in function, a gas delivery system is added in order to supply a chemical compound just above the sample and directly in the path of the ion beam. The gas, usually an organometallic compound, is adsorbed onto the sample surface. This precursor is then struck by the gallium ion beam (and additionally by some secondary emission products), causing it to decompose as its bonds are broken. The volatile organic impurities are released and removed by the FIB's vacuum system. The desired metal, say platinum, is heavy enough to remain deposited on the surface, creating a thin film that can act as an electrical conductor (figure 7).

Although the chemical deposition just described is the predominant method of deposition with the FIB, there are two others which in certain situations may be advantageous. The first method, direct deposition, uses large diameter beams with low energy to deposit thin films, usually of gold. Low energy microbeams need very small currents and are very slow. The other alternate deposition method is nucleation with chemical vapor deposition (CVD), usually used to deposit carbon, aluminum, and iron. As an extension of chemical deposition, this technique uses the same gas injection system to create nucleation on the substrate. Once that is done, CVD is used to grow a thin film in the nucleation regions. The main advantage of this method is that it produces a film of uniform height [8].

Once again, when an organometallic gas such as  $W(CO)_6$  is introduced in the area of the ion beam, the ion beam can be controlled to decompose the molecules which adsorb onto the surface and form a metal layer. This metal conduction layer can function as a probe pad or be used to make a new connection for nano-circuitry. Unfortunately, the film is often impure, causing a high resistivity. Long wiring runs requiring lower

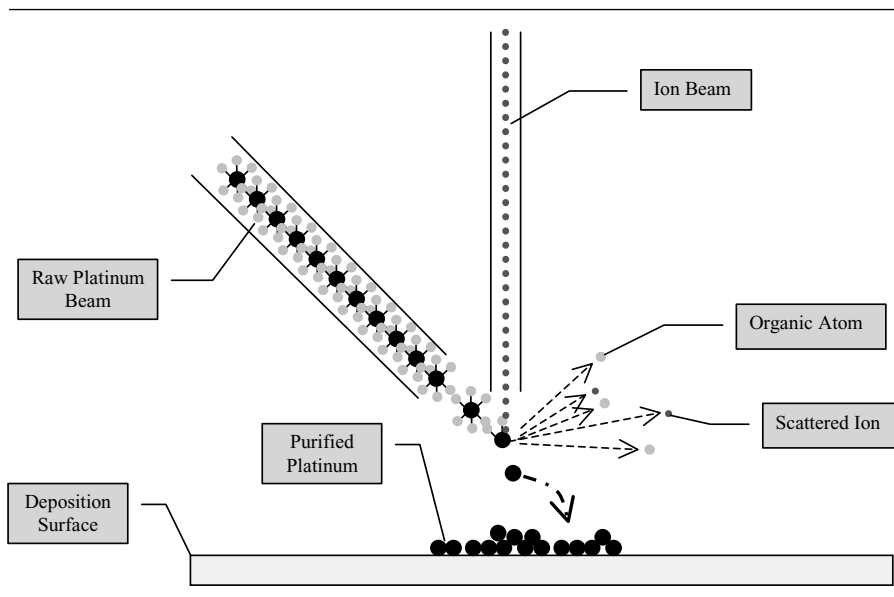


**Figure 7.** Schematic diagram of the platinum deposition process.

resistivity can be achieved by combining FIB local connections with long laser CVD deposited gold conductors. In this technique, a gold carrier gas is decomposed by a scanning laser beam, leaving a 5–10  $\mu\text{m}$  wide gold line on the work surface with a relatively low sheet resistance. In addition, just as it can deposit a conducting thin film, the FIB can be used to deposit a high quality oxide insulator. A siloxane type gas and oxygen are introduced into the path of the ion beam at the impact area. Decomposition of the complex silicon bearing molecule in the presence of oxygen leads to absorption into the surface and formation of a silicon dioxide insulator layer. With the aid of oxide deposition, the re-insulation of cut IC wiring and FIB deposited conductors is now possible, making complex multilevel wiring repair practical.

The FIB deposition system, although very useful, is not perfect. In general, the cracking of the organometallic molecule is not complete, leaving some organic impurities deposited in the thin film. In addition, some lingering gallium atoms can hurt the insulating ability of a deposited layer. Still, although CVD deposits are often more pure, the advantage of using the FIB system is its ability for precise, localized deposition, and its capacity for controlling the different heights of the depositions. Even so, the use of ion beams may not always be ideal; research has shown that in certain cases, electron nanofabrication has been able to match the work of the ion beam without the impurities that come along with using the FIB [9].

Nevertheless, the FIB is unparalleled in its patterning capability. By adjusting parameters of time, gas flux, and ion current, it allows deposition of three-dimensional structures with complete control over size, position, and height. For example, Khizroev, *et al.*

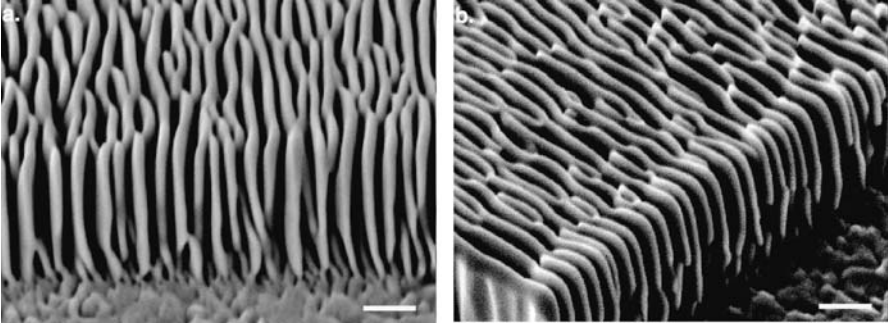


**Figure 8.** SE images of a two-beam FIB fabricated Pt nano-fin structure on Si surface, where (a) and (b) are viewed from different directions (scale bar: 0.3  $\mu\text{m}$ ) [11].

have successfully deposited non-magnetic tungsten at the nanoscale range to aid in the fabrication of nanomagnetic probes [10]. In addition, we have performed experiments with ion-beam induced deposition of self-assembled nanostructures using a technique that formed nanoscale hollow bulk structures. These nanofins were deposited perpendicular to the substrate (figure 8) [11]. Using deposition in combination with its milling capabilities, the FIB can accurately build almost any nanostructure, a feature which is invaluable in today's research.

### 2.5. Implantation

Another critical feature of the FIB system is its ability to produce maskless ion implantation, a technique fundamental in the fabrication of semiconductor devices. In traditional semiconductor fabrication, ions are allowed to bombard the entire wafer, and regions which are not to be implanted are covered by a patterned film, or mask [3]. With the FIB, whose level of localized control and specificity has already been discussed, we now can discard the mask and simply aim the beam at the areas where implantation is desired. This provides new abilities to control gradients in doping and the control the depth of the implantation [3]. Like many of the other capabilities of the FIB system, its use for ion implantation will minimize costs, both in time and money.

Ion implantation has been used for materials modification as well. In general, defect formation following ion implantation plays unpleasant roles when using the FIB system, but occasionally it can have a positive effect. For example, recent experiments have shown that implanted atoms can be induced to self-assemble into nanoclusters through thermal annealing or radiation. To understand these properties, a Monte Carlo model has been developed with the ability to simulate diffusion, precipitation and interaction kinetics of implanted ions [12].

With all its advantages in accuracy and precision, an almost directly related disadvantage in using the FIB for ion implantation is its slow processing rate. Even so, there

are situations where this rate is not an issue, and in these cases, the FIB becomes an crucial tool.

## 2.6. Imaging

Although we have already discussed some aspects of FIB imaging, they are worth repeating and expanding upon. Again, the method used in FIB imaging is similar to that in the SEM, except that the incident particles are ions instead of electrons. When the ion beam strikes the sample surface, one of the resulting processes is the emission of secondary particles, including low energy secondary electrons, neutral atoms, secondary ions, and photons. In general, the most prevalent among these emissions is secondary electrons, whose signal is usually used to obtain the image. In some cases though, images can only be obtained from secondary ion signals [13].

As mentioned earlier, imaging resolution below 10 nm is possible with the FIB, but what makes FIB images particularly useful is their ability to display detailed surface topography. The key mechanism for displaying topographic contrast is the fact that the emission rate of secondary particles (ions or electrons) will vary with the angle between the incident beam and the normal to the surface of the sample. Since the FIB has a shallow penetration depth relative to an electron beam, particles are generated from only a limited portion of the sample, and therefore the FIB allows much higher surface sensitivity, and in some cases is able to display a more detailed topographical map [4, 13].

In addition to topographical contrast, another merit of FIB imaging is its ability to contrast between grounded conductors and insulating areas or isolated conductors. The incident  $\text{Ga}^+$  ions will place a positive charge on the insulating or isolated conducting surface areas, suppressing the yield of secondary electrons collected for imaging from these regions. Insulators and isolated conductors will therefore appear darker in the images, while grounded conductors will be bright. Although moderate surface charging can enhance voltage contrast in ion beam images, too much charge can severely depress secondary electron emission, and so with insulator surfaces, secondary ions are often used to obtain the image. In general, the voltage contrast imaging technique is useful for locating failure sites in devices as well as detecting endpoints when etching (figure 9), making the FIB an attractive tool in many integrated circuit applications [14].

The FIB system is also proficient in providing materials contrast. This results from the fact that different materials produce different yields of secondary particles because of the complex way the ion beam energy is lost within the sample. Materials contrast is frequently the dominating effect in FIB images. It is worth mentioning that the yield of secondary ions from metallic surfaces is greatly increased by the presence of oxides or carbides, making these regions much brighter. This property gives the FIB applications in studies involving corrosion or grain boundary oxidation of metals [4].

The last type of contrasting we will mention is channeling, or crystallographic orientation contrasting. Some of the incident ions are “channeled” down between the lattice planes of the specimen, with the penetration depth depending on the beam

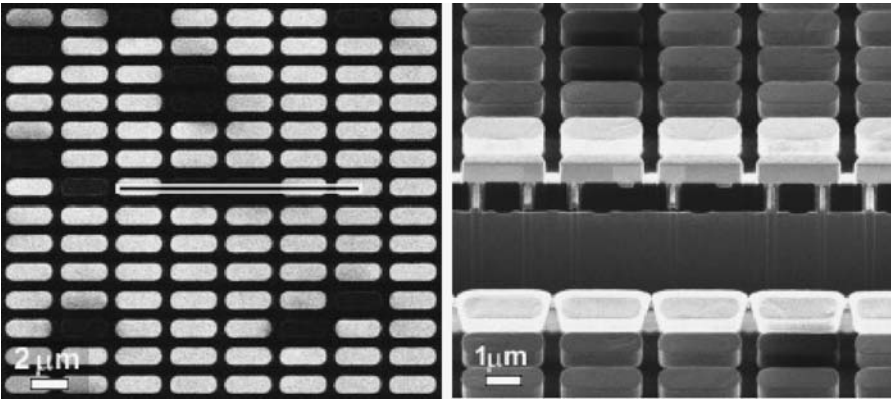


**Figure 9.** Voltage contrast reveals open via positions in a contact chain structure. The cross-section image at the position of the line (right) shows deep etching of the vias. (Courtesy of IMEC)

current, the relative angle between the ion beam and the lattice plane, and the interplanar spacing of the lattice. Channeled ions yield fewer secondary particles, causing the channeling grains to appear darker in FIB images. This technique is often used in monitoring the grain size distribution within Al-Cu films as well as in the study of electromigration effects in metallization [13, 15].

In conjunction with the high resolution picture, the FIB can be equipped for secondary ion mass spectrometry (SIMS), which allows detailed elemental analysis (figure 10) [16]. With this and the various contrasting techniques discussed, the FIB can produce an elemental map with a nearly complete set of vital data for almost any microscopy application.

### 2.7. The Two-Beam System

So far, we have focused on the properties and capabilities of the FIB system, and certainly a plethora of applications can be derived from these capabilities alone. Still, by combining the FIB's imaging and sample interaction abilities with the SEM's high resolution, non-destructive imaging, new heights in microscopy research can be achieved. The two-beam system accomplishes just that; by putting FIB and SEM technology together in a single machine, the two work symbiotically, achieving tasks beyond the limitations of either individual system.

In a two-beam system, the ion beam and electron beam are placed in fixed positions, with the former coming in at an angle (figure 11). The two beams are co-focused at what is called the "coincidence point," typically with a 5 mm working distance; this point is an optimized position for the majority of operations taking place within the machine. For best performance, the ion beam is tilted  $45^{\circ}$ – $52^{\circ}$  from the electron beam, allowing SEM imaging and FIB sample modification without having to move the sample. In addition, the stage can be controlled to tilt, allowing changes in the



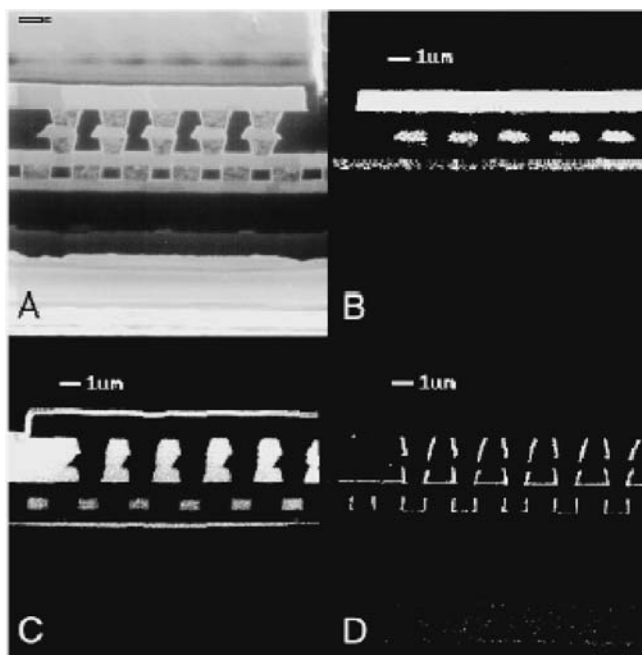


**Figure 10.** Chemical map of a cross-sectioned face of an IC. (A) FIB secondary electron image. (B) Mass 27 Al. (C) Mass 28 (Si). (D) Mass 48 (Ti). The maps are  $256 \times 256$  pixels. Primary beam current = 40 pA [16].

sample-beam orientation. As with the FIB system, the two-beam can be controlled using integrated software with a single user interface.

Within the two-beam system, the FIB and SEM complement each other perfectly, providing new advantages which can simplify and improve microscopy research. For example, FIB imaging is very useful because of its high contrasting abilities, but it can cause damage to the sample. The SEM, on the other hand, has relatively lower contrast, but its images have higher resolution, and its use will not damage the sample. Depending on the specific needs of the user, the FIB, SEM, or a combination of the two can be used to obtain whatever imaging data is required. For example, in a study done at Portland State University, both the FIB and SEM were used to image and characterize carbon nanotubes, each providing useful information [17]. Similarly, reconstruction of 3D structure and chemistry of a sample will be simplified by the use of the two-beam system, as this technique is achieved by interpolating the 2D SEM/FIB images and ion-assisted SIMS chemical maps of successively exposed layers milled by the ion beam [18].

In addition to the combined imaging benefits, the two-beam system allows precise monitoring of FIB operation through the SEM. By using the slice-and-view technique for observing the progress of an ion-beam cross section, the operator can precisely stop

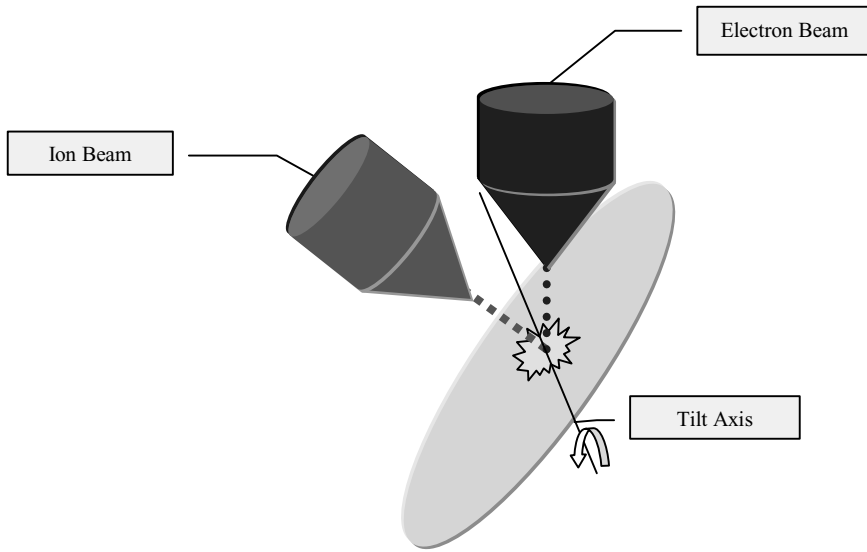


**Figure 11.** Schematic diagram of two-beam system.

the milling process at any point to obtain local information. Furthermore, state of the art technology now allows us to use the ion beam and electron beam simultaneously without interference, eliminating the trouble of switching back and forth. In the “CrossBeam” system, the sample can be imaged in real time with the SEM while the FIB is being used, giving the operator complete control over the milling process. This provides even higher levels of accuracy when creating cross-sections [19]. The SEM’s damage-free monitoring is especially useful in the final phase of TEM sample preparations. It solves the dilemma found when using the FIB system alone, where the only way to observe the process is ion imaging, which can damage the sample. In a successful physical localization of IC fails, Zimmermann et al presented a completely in-situ two-beam technique that combines SEM monitored ion milling,  $\text{XeF}_2$  staining and SEM imaging [20].

When dealing with charge neutralization, the two-beam system once more eliminates a problem encountered in the FIB. In general, when a sample is flooded with positively charged ions, the surface becomes charged, hurting the resolution of the image. With the availability of the electrons from the SEM, this problem is trivial. Similarly, a negative surface charge could be combated using the positively charged ions.

Another capability of the FIB machine, deposition of metal or insulating layers, can also be improved using the two-beam system. In some cases, using the ion beam for insulator deposition may lead to a material with poor insulating properties because of the high amount of gallium incorporated into the layer; when this is a problem, SEM induced deposition can be used, ensuring high insulating quality. In the case of

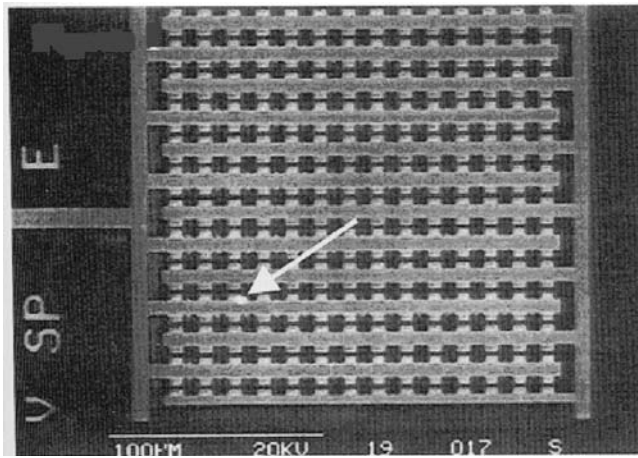


**Figure 12.** EBIC “hot spot” signal superimposed on secondary electron image showing one leakage site on this test structure [22].

$\text{SiO}_x$  pads deposited by the SEM, it has been found that the resistance of the layer is two orders of magnitude higher than when using the ion beam [21]. In addition, while attempting to localize IC fails, this time electrically, Zimmermann *et al.* used the electron beam to deposit a highly insulating  $\text{SiO}_x$  layer in-situ in the two-beam system. A Pt probe pad was then deposited on the insulating  $\text{SiO}_x$  layer with ion beam assistance [22]. As before, the combination of FIB and SEM systems has proved both practical and valuable.

Finally, the SEM brings with it to the two-beam system an electron beam induced current (EBIC), a feature not present in the individual FIB system [23]. This is a useful technique for locating defects in diodes, transistors, and capacitors. The SEM beam generated a characteristic electron flow signal in the sample, which is then collected and amplified, providing an EBIC “hot spot” image (figure 12). This is powerful in pinpointing the bad site in a device that may contain as many as a few hundred thousand structures. Since the FIB can be used to prepare the sample for EBIC characterization and then to further analyze the located failure site through precision cross-sectioning, the two-beam has an advantage above the SEM alone.

We have seen now that the two-beam FIB system is an excellent multifunctional tool for sample imaging, modification and analysis. It offers high resolution 3D non-destructive imaging with the electron beam, as well as useful contrast imaging and SIMS chemical mapping with the ion beam. It can carry out precise, highly controlled an automated sample modification including ion milling, lithography, micro-machining, gas-assisted etching, and deposition. With all these and other capabilities, it is no question that the two-beam system will have an even longer list of applications. The remainder of this review is devoted to highlighting some of the most important of these applications.

### III. APPLICATION OF FOCUSED ION BEAM INSTRUMENTATION

Thus far, we have discussed in depth the tremendous power of the FIB machine, with its wide-ranging functions and capabilities. Yet the capabilities by themselves are not the direct reason for the great industrial interest in FIB technology; instead, it is the abundance of applications yielded by these capabilities that have given rise to excitement. These applications seem to come with a promise of commercial success, and will therefore be discussed in detail in this review. We will begin with applications related to surface structure modifications, then look at the popular application of TEM sample preparation, and finally go over the imaging applications found in the FIB machine.

#### 3.1. Surface Structure Modification

As discussed in earlier sections, the focused ion beam has the capabilities of a milling tool at micro and nano scales, making it an attractive new technique for micro-machining among other tasks. Three industrial fields particularly stand out as ideal candidates for the application of this ability in the FIB system. It is an almost perfect fit for the integrated circuit industry, and its need for more precise failure analysis and modification of its products. The FIB provides engineers with a tool for defect location and investigation, defect sample prep, circuit rewiring, and surface modification, all vital in circuit design and fabrication. In addition, the FIB holds lithographic capabilities that are becoming more and more effective. Critics have questioned the speed of the FIB system for patterning and lithography because of its serial nature, but studies have shown not only that FIB is up to par with lithographic standards, but also that FIB lithography and patterning have proven effective with numerous materials and specific applications.

Of course, as with any new technology, it is important to study its limitations. With the FIB, there is interest in knowing what surface modification at low ion dosage will do. At the Oxford University Department of Materials, a recent study was done to characterize low-dose ion beam surface manipulation. A Si wafer was bombarded with  $\text{Ga}^+$  ions at different doses between  $10^{13}$  and  $10^{19}$  ions  $\text{cm}^{-2}$  (where the dose =  $(I_{\text{ion}} * t_{\text{exposure}}) / (A_{\text{pattern}} * 1.602 \text{ E}^{-15})$ ). Rectangles with depths varying around 4 nm and dimensions of  $4 \times 1 \mu\text{m}$  were created and investigated, along with grids consisting of lines  $5 \mu\text{m}$  by 20 nm. Atomic force microscopy was then used to characterize the topology of the altered surface. It was discovered that the results differed for varying doses of ions. In almost all cases, edge protrusions were noted, ranging from 0 nm ( $10^{13}$  ions  $\text{cm}^{-2}$ ) to a maximum height of approximately 1 nm, when below a dosage of  $10^{17}$  ions  $\text{cm}^{-2}$  (figure 13). Edge effects were blamed mainly on  $\text{Ga}^+$  implantation from stray ions that would unintentionally deposit in nearby regions, as well as redeposition of secondary and backscattered material [24].

With the knowledge we have from this and other research, we can understand the limitations of the FIB system and work within these limits to achieve successful applications of this valuable technology.

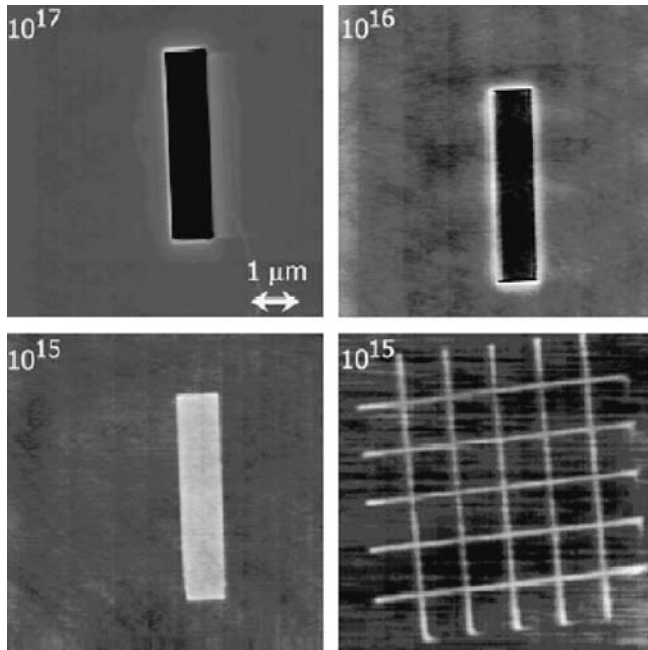


**Figure 13.** AFM image of features produced by low dose  $\text{Ga}^+$  ions on Si. Note the protruding edge effect on  $10^{16}$  ions  $\text{cm}^{-2}$  dosage (top right) [23].

### 3.1.1. Integrated Circuit Analysis and Modification

The semiconductor industry has made tremendous use of the FIB machine for its applications in defect analysis and modification of integrated circuits during the prototype stages. The benefits of being able to both remove and deposit material can be directly observed, as the ion beam is capable of milling away enough to cut a wire while depositing conducting material in another area to connect two pieces of wire (figure 14). All this is done with minimal damage to the wafer itself, allowing for the test product of be continually improved. The FIB can easily be used to create samples of the wafer for further analysis.

Unfortunately, when investigating integrated circuits for defects, it is often difficult to find the specific area of interest because of the lack of visible signs on the surface of the material. As good of a repair tool as the FIB may be, the failure cannot be repaired if it cannot be found. This problem has been analyzed at FEI Europe, Ltd. and a technique has been developed to effectively locate the area of concern utilizing the FIB machine for the entire process. The group examined a transistor containing a certain gate (approximately  $1\mu\text{m}^2$ ) under which a thin gate oxide layer had broken down due to excessive voltage application (figure 15). The source and drain lay on opposite ends of the gate, which sat on top of the gate oxide layer, all of which resided on a silicon substrate. TEM samples of the failure site ( $<100$  nm in diameter) were

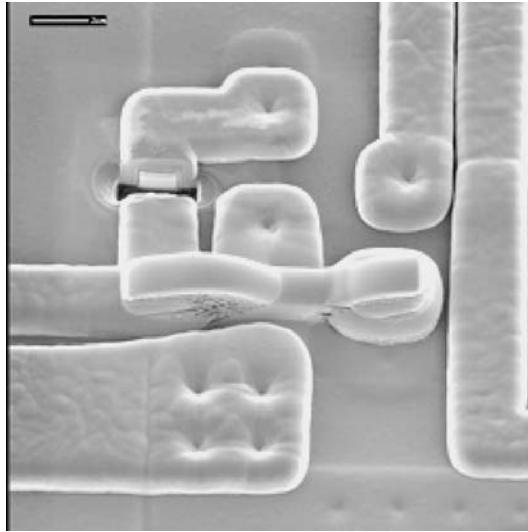


**Figure 14.** Image of rewired circuit. (Courtesy of Integrated Reliability)

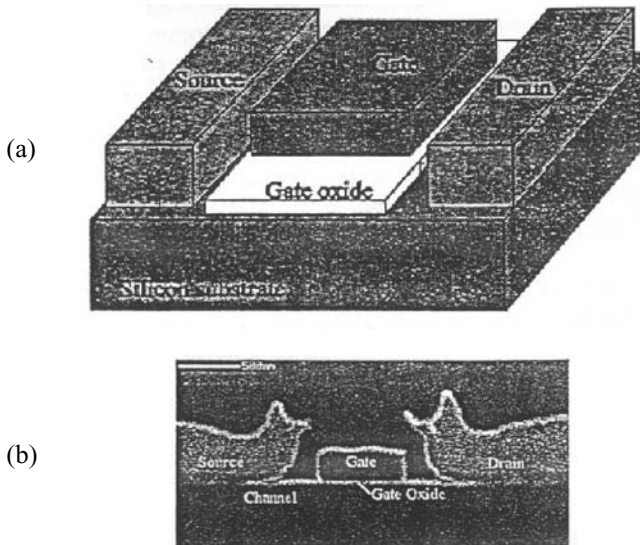


**Figure 15.** (a) Transistor Structure (b) Image of defect, where the break is clearly visible [24].

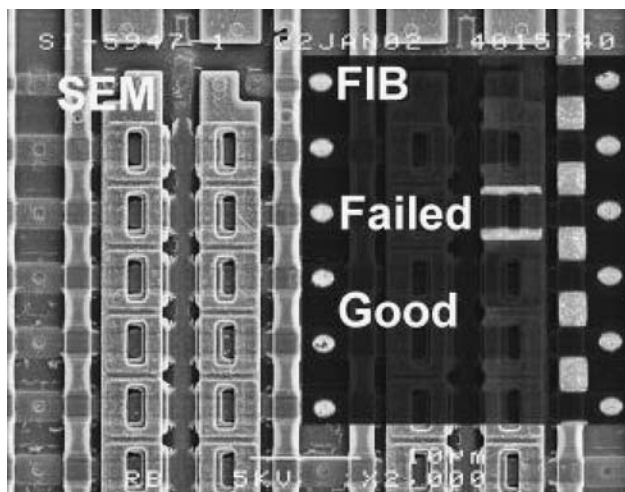


**Figure 16.** Combination SEM and FIB passive voltage contrast images. The FIB portion (at the right) shows an area of memory cells after exposing the wings of the floating gates. One floating gate appears bright, indicating that it is grounded and therefore the tunnel or gate oxide has failed [25].

desired for investigation on the mechanics behind the problem, but the area of failure had to first be located. By starting on high beam currents, an outline and subsequent trenches were dug around the region thought to be of focus. Removal of thin slices together with fast imaging was performed until the structure became apparent. Once achieved, low beam currents were used to uncover the region, noting that all focusing and stigmation adjustment were done away from the region. It was found that these basic steps succeeded in efficiently locating an area of defect [24]. Again, once the defect is located, the FIB's capabilities make it an ideal tool for use in integrated circuit modification.

Other work, reported by Haythornthwaite *et al.*, shows the versatility of the FIB system and its wide range of circuitry applications. The group worked with electrically erasable programmable read only memory, which after extensive use experiences failures. The FIB machine proved useful in three stages of the failure analysis process. Initially, using the FIB in passive voltage contrast mode helped confirm the occurrence and location of the failures (figure 16). Then, as an added benefit, the FIB was able to identify weak storage transistors on the memory device, which if not taken care of could soon lead to other failures. Finally, TEM samples were created using the FIB system, a process which will be discussed in depth in a later section [25].

### 3.1.2. Lithography and Patterning

Another application of the FIB machine related to surface modification involves its lithographic capabilities in nanofabrication. It holds clear advantages over other methods in its ability for high resolution patterning and depth of focus, and therefore should

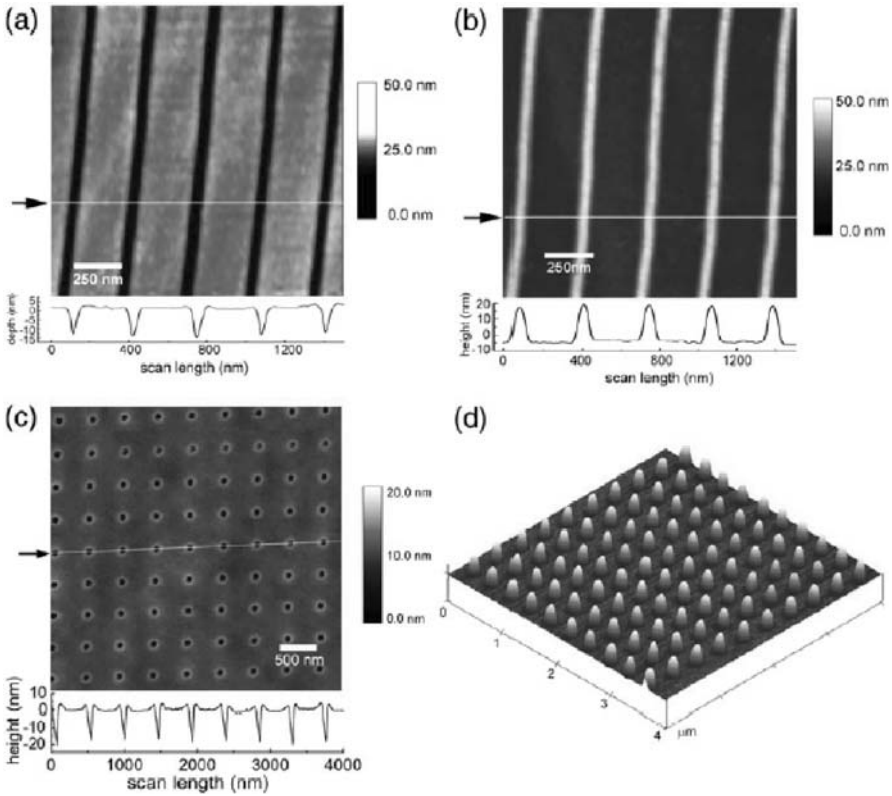


**Figure 17.** AFM images of FIB patterning. On the left are the actual FIB cuts, and on the right are their PDMS replicas [26].

be studied as a practical alternative. Unfortunately, because of the precision of the FIB system and the detail of lithography, this application of the FIB has one major drawback; although producing high quality results, the FIB machine appears unable to perform high throughput production. This problem was studied in depth at the University of Cambridge, where Li *et al.* replicated FIB created structures with nanocontact imprinting. Silicon wafers were patterned ( $10\ \mu\text{m}$  single pixel line and  $20\ \text{nm}$  diameter dots) with a  $30\ \text{kV Ga}^+$  ion beam at currents of 1, 4, 11, and  $70\ \text{pA}$ . Analysis was done using the AFM and replicas were made by pouring polydimethylsiloxane (PDMS) over the print master, then peeling it off (figure 17). Dwell time, ion dosage, and beam current were characterized, and satisfactory molds were created on almost all accounts [26].

As a result of its slow rate of progress, the FIB system, though proven capable of lithography, is still often criticized. With patterning rates generally around  $0.1\text{--}1\ \mu\text{m}^3/\text{nC}$  incident ion current, its limited ability has been deemed as a restriction in the applicability of FIB. However, Liu *et al.* have reported the ability to rapidly



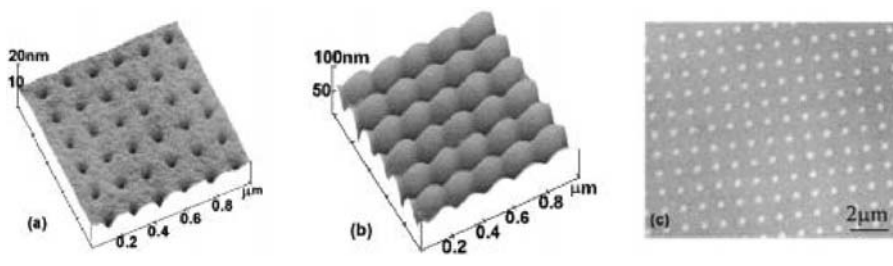


**Figure 18.** AFM images of topography in PMMA following FIB exposure at (a) 1 pA beam current and a total irradiation time of 20  $\mu\text{s}$ /feature, (b) 11 pA beam current and a total irradiation time of 500  $\mu\text{s}$ /feature. (c) TEM image (recorded at 200 kV, using mass–thickness contrast with an objective aperture, including just the transmitted beam of an array of sputtered features created using an 11 pA beam and a total irradiation time of 5 ms per feature). Samples were prepared by direct spinning of PMMA films onto TEM grids coated with thin (5 nm) amorphous C films [27].

create features, at rates exceeding those of past methods. Patterns were created on polymethylmethacrylate (PMMA) that was spun onto Si wafers, producing a 120 nm thin film (figure 18). Using a  $\text{Ga}^+$  ion beam with beam currents varying from 1–70 pA, features were created with sizes ranging from 60–200 nm in diameter and 5–30 nm in depth. At diameters of 60 nm and depth of 5 nm, the paper reports milling times at 20  $\mu\text{s}$  per feature and a material removal rate of 1000  $\mu\text{m}^3/\text{nC}$ . Other features were also created at rates orders of magnitude faster than previously reported. One point of particular interest was the fact that all sputtering yields were consistently unusually high. The group proposed the possibility that this was the result of a depolymerization of the polymer being etched that was aided by the ion beam, a phenomena generally seen at higher temperatures [27]. This is only one of several cases of successful high speed lithography using the FIB. Although this method may not be the best in all situations, there are clearly cases when the FIB is the best tool, both in speed and quality, for lithographic and micro-printing applications.

Recently, a group at the University of Limerick in Ireland developed a two step negative resist image by dry etching (NERIME) process for lithography. The method combines exposure to  $\text{Ga}^+$  ions from the FIB machine with reactive ion etching (RIE). By doing so, the group has further strengthened their abilities beyond those of conventional lithography, as the process eliminates some of the limitations of basic FIB lithography, such as low penetration depth and sample damage [28].

### 3.1.3. Materials Characterization and Alteration

We have already discussed in depth the characteristics of the FIB system which make it excel at material characterization and alteration. Again, its milling and deposition abilities allow the creation of almost any three-dimensional microstructure (figure 19), and its cross-sectioning capability proves to be very useful in the study and characterization of materials. As a result, there is a seemingly endless list of applications that can be derived from the FIB system. We discuss here just some of the many studies done

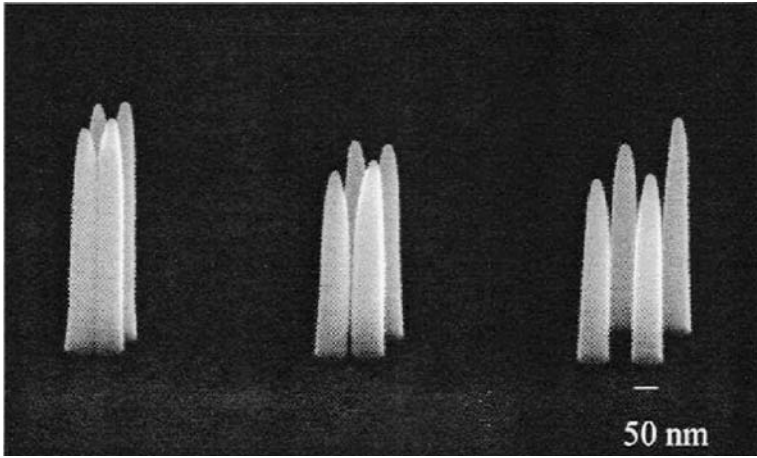


**Figure 19.** Creation of nanometer 3D structures. (Courtesy of FEI Company)

with the FIB into materials characterization and alteration. As with any new machine, there is an interest in finding out new processes and techniques that improve the old ones, as well as an interest in new information that can be gathered. This section serves to highlight some of these studies.

Gallium Nitride (GaN) is a widely applicable semiconductor material that has a high melting point and strong light sensitivity properties, which make it well suited for both high temperature devices and light detecting or emitting devices [29, 30]. Unlike traditional methods of etching, the FIB does not need an etch mask for manipulation because of its local specificity and precision; this is a most valuable feature in semiconductor fabrication. In a study done at the University of Bristol, FIB etching onto GaN structures was studied with both AFM and SEM techniques. Using an FIB machine with a gallium ion gun as well as a magnetic sector mass analyzer, a 20 nm  $\text{Ga}^+$  ion beam was used to etch square patterns of  $49 \mu\text{m}^2$  onto a 1.2  $\mu\text{m}$  thick GaN specimen at doses of 500, 1000, 1500, and 2000  $\text{pC}/\mu\text{m}^2$  (all done without an etch mask). Images were obtained from the SEM using a secondary electron detector, as well as performing a SIMS analysis. The etch depths and surface roughness were closely studied, and it was found that the etch rate increased linearly with ion dose, which in turn resulted in an increase in etch depth. The edge sections were found to have a roughness below 0.1  $\mu\text{m}$ , a quite favorable number. All in all, it was found that although slower than traditional methods, FIB etching on GaN proved to be more advantageous in its high quality production and versatility [30].

In other experiments, it has been shown that ion bombardment on hydrogenated silicon-carbon alloy films ( $\text{a-SiC:H}$ ) creates optical contrast between crystal layers (differentiating between those bombarded and those not) (figure 20). This is of great interest because having a large optical contrast in  $\text{a-SiC:H}$  will result in a good material for opto-electronic devices as well as for difficult environmental conditions. A

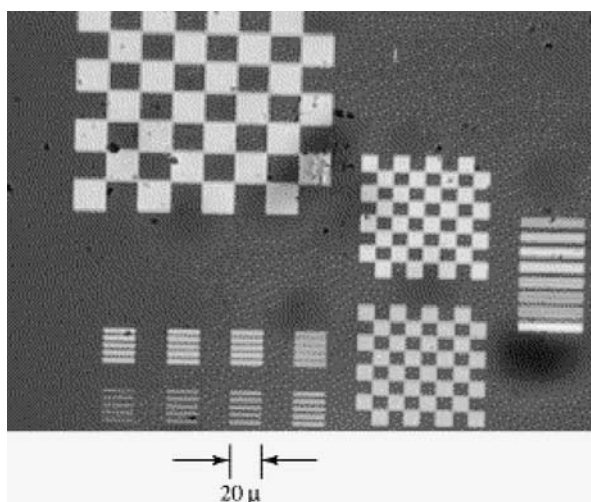


**Figure 20.** Optical contrast pattern written into a GD a-Si<sub>0.85</sub>C<sub>0.15</sub>:H film deposited on Corning 7059 glass substrate. The transparent and opaque regions represent unimplanted and implanted parts of the film, respectively. The patterning has been performed with the help of a program-controlled Ga<sup>+</sup>-focused ion beam. The minimum feature size is 2.5 μm.

recent study compared Ga<sup>+</sup> and Sn<sup>+</sup> bombardment with previous experiments using As<sup>+</sup>. Films were prepared with two methods, one being a glow discharge technique (GD), and the other reactive magnetron sputtering (SP). Samples were bombarded at 50 keV (Ga<sup>+</sup>) and 60 keV (Sn<sup>+</sup>), with an ion-beam intensity of 2 μA/cm<sup>2</sup> and doses between 10<sup>15</sup> and 10<sup>17</sup> ions cm<sup>-2</sup>. In both cases, huge increases in optical absorption coefficients were noted as compared to previous experiments with As<sup>+</sup>, indicating that the formation of optical contrast was much more prevalent. Although strong in both cases, this effect was even greater in the GD films as compared to the SP films [31].

Furthermore, the extent of the FIB's material altering capabilities, particularly when part of an integrated two-beam system, was demonstrated in work done by Anzalone *et al.* in creating complex 3D structures. They show that using the milling and deposition techniques discussed earlier, it is possible to model structures based on software defined inputs or bitmap files using a digital patterning generator. Computer Aided Design (CAD) files were used in conjunction with ion beam assisted CVD to create 3D helical structures (figure 21) [32].

In addition to alteration, many experiments have shown that the FIB machine is a great tool for the characterization of nanosized objects. For example, we expanded the applicability of the FIB by using it in combination with high-resolution strain mapping software. These two techniques, when used together, provide a new method for in situ measurement of the residual stresses in thin films. First, the FIB system is used to create narrow slots having precise location. These slots serve to relieve residual stress, causing the surrounding film to displace. The strain mapping software is then

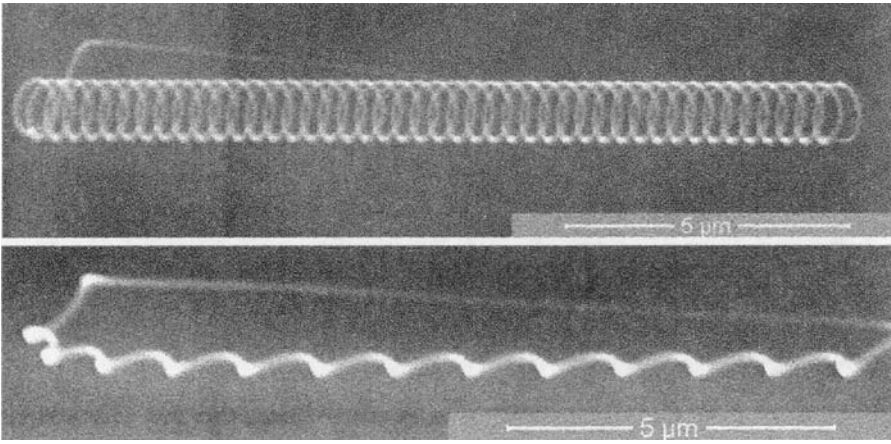


**Figure 21.** SEM images of an electron beam deposited Pt helical feature obtained with the use of the digital patterning generator [32].

used to measure these displacements and relate them to the residual stress (figure 22) [33]. Clearly, the FIB system is not only a useful stand-alone machine, but that it also complements other techniques, making them more efficient and of a higher quality.

In a different experiment, we studied the lubricated wear of steel couples coated with W-DLC. Among the methods used to characterize the samples, the two-beam FIB system was used to reveal the sub-surface condition of the coating and substrate. The ion beam was used to make small sections at specific locations, which were then observed using the electron beam (figure 23) [34]. Similarly, the FIB was used to characterize sub-surface damage in a study of foreign object damage (FOD) in a thermal barrier system. The conditions were set to simulate those of a turbine engine, and the FIB observations indicated damage in the thermal barrier coating (figure 24). The study demonstrated that these changes were caused by particle impact, confirming the presence of FOD [35]

These are, of course, only a few examples of the tremendous applicability of the FIB system for the alteration and characterization of materials. With all its uses, the FIB has become an invaluable tool for nanotechnology research.

### 3.2. TEM Sample Preparation for Imaging and Analysis

Perhaps the most studied and commonly used application of the FIB is for transmission electron microscopy (TEM), specifically in sample preparation, where the FIB provides revolutionary methods of creating electron transparent samples [36–41]. The TEM is very useful for finding information on the atomic structure and composition of solid materials. As its name suggests, the TEM collects its data from electrons that are transmitted (or diffracted) through the sample. Therefore, TEM samples must be extremely thin, with optimal samples less than 50 nm thick and an maximum near

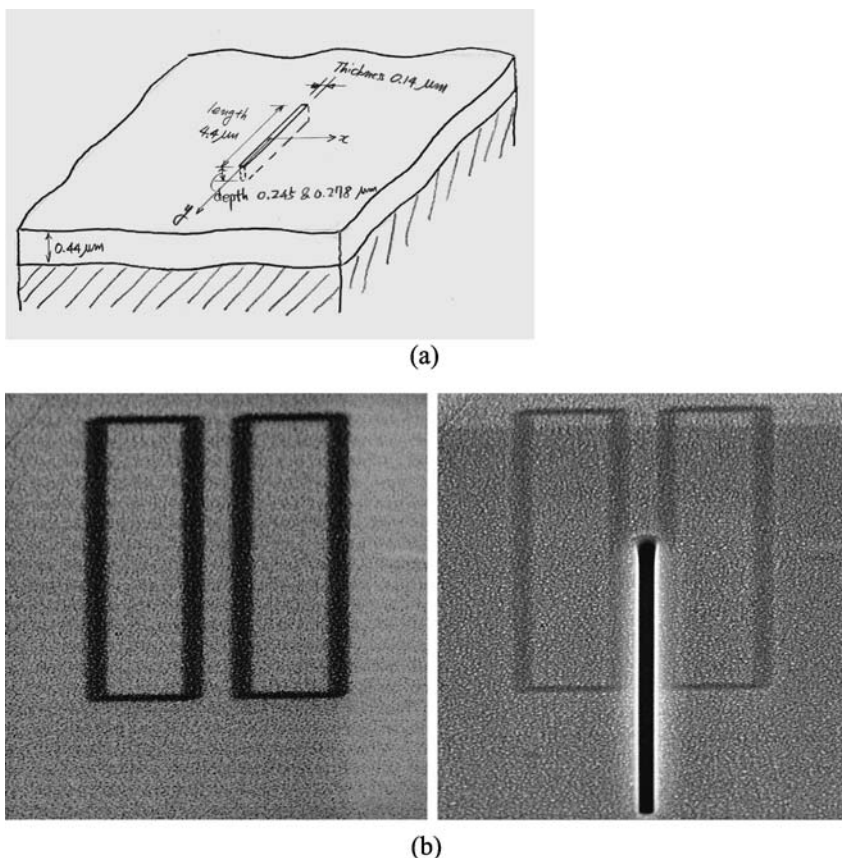


**Figure 22.** (a) A schematic of a FIB slot introduced into a film, defining the coordinates. (b) SE images of a region of a diamond-like carbon film before and after the introduction of the FIB slot [33].

200 nm. In addition, it is quite necessary to have a sample which has been cleanly extracted from the bulk specimen because of the fact that defect analysis (a major use of TEM) is so location specific. In the past tedious time consuming techniques for producing samples such as grinding and polishing were constantly a limiting factor in the progression of research. In recent years however, the focused ion beam machine has shown vast improvement in the time and quality of sample preparation.

The FIB holds a number of advantages over previous methods for TEM sampling. For example, since the sample can be rotated and oriented without ever having to take it out of the chamber, much time is saved while digging or etching the sample. The defective area can be found by thinning away at different areas until the defect is located, and then the milling process can begin. Also, samples can be much more precise in their overall shape and size due to the exactness of the FIB. Lastly, the FIB lets the user watch as he or she is sectioning a sample, allowing for much better

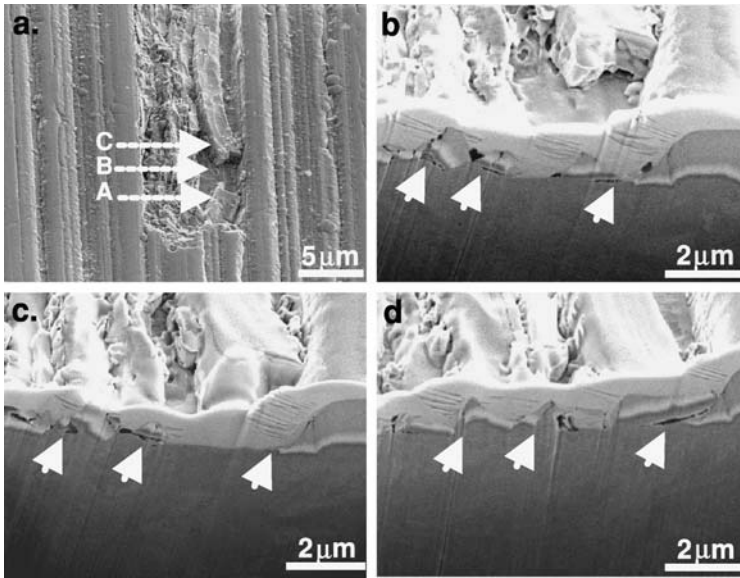


**Figure 23.** (a) SE image of surface morphology of damaged area. (b–d) SE images of FIB cross-section of W-DLC coating at ‘A,’ ‘B,’ and ‘C,’ respectively. The arrows identify regions where the retained W-DLC coating segments have either translated or rotated [34].

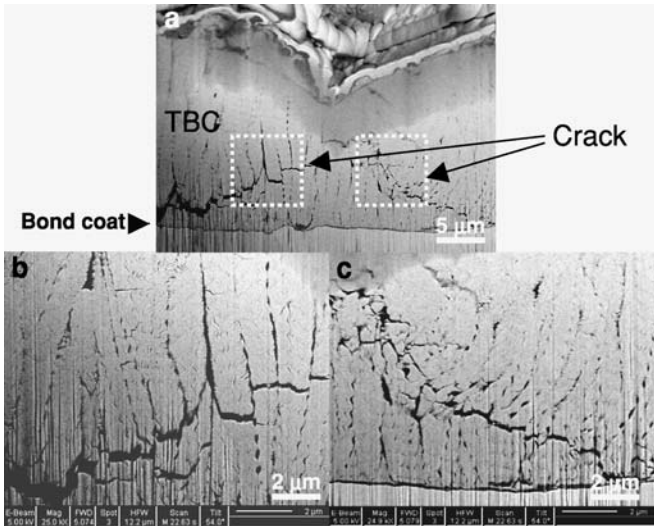


**Figure 24.** SE image of FIB cross-section showing the kink band beneath the impact site. The cracks, magnified in (b) and (c), extend along the kink band from the densified zone to the TGO layer [35].

decision making. This feature is greatly enhanced with a two-beam FIB system, where the SEM can be used for high-resolution imaging. In general, the FIB's capabilities of precise cutting and polishing give it a unique ability to quickly create excellent TEM samples, a process which once needed numerous machines to take care of. Cairney, *et al.* have taken advantage of this, using the FIB to create sample of “large, uniformly areas with relative ease” for their TEM work studying TiN and TiAlN thin films [37]. Similarly, Volkert *et al.* used the FIB to prepare TEM samples for their work on synthetic fluorapatite-gelatine composite particles. They report that the FIB-prepared samples make “high-quality, crack-free specimens with no apparent ion beam-induced damage” [38].

The most practical method for sample creation is the so called lift-out technique, where the focused ion beam, with its massive density, is able to perform site specific milling on bulk samples. The samples are generally coated ahead of time with some conducting metal so as to eliminate charging, and are then placed in the FIB machine for alteration. Once secured in the chamber, the region of investigation is found and a trench is dug around the area in a step-like fashion. It should be noted that the X and Y dimensions of the rectangular trenches must be at a ratio of 2:1 respectively so that one is able to image the entire trench. When the sample is thin enough, it is basically cut along the attached edges and lifted out with a glass rod, then placed in the TEM grid for analysis (figure 25). The lift-out technique was used by Wang *et al.* to prepare CMOS cross-sectional specimens starting with integrated circuit wafers. They report success in producing a “large and uniform sectional specimen in a very short time.” On the other hand, they mention a disadvantage of the lift-out technique, namely that a finished specimen cannot be refabricated if it is too thick; newer techniques using the FIB have been able to overcome this problem [39, 40].

Another significant problem which has been observed to occur during thinning in the lift-out method is a warping effect in the sample. As thinning occurs (to roughly less than 200 nm), stressed samples fall into a bent shape to alleviate the pressure (figure 26). Stress can be caused by the bulk sample because of poor mounting or can be the result of the internal structure of the material. In either case, a study done at FEI Europe Ltd. found that cutting either one or both of the edges (depending of the seriousness of the warping) of the near fully thinned sample would alleviate the stress by giving it room for relaxation. This technique has proved to solve almost all cases of warping problems [41].

An alternative to the lift-out method of TEM sample preparation is called micro-pillar sampling. This technique is particularly useful in preparing specimens in situ for the scanning transmission electron microscope (STEM). The FIB micro-sampling method is used to extract a pillar shaped sample from the specimen, which is then mounted on top of a conical stage developed specifically for this method. The sample is then transferred to the STEM, where various imaging techniques are used [40].

In addition to material science, the FIB machine's success in TEM sample preparation has been used for environmental science applications. Copper run off from the roofs of many buildings is becoming a serious environmental concern, and strategies to reduce infiltration are being explored. One such idea has been to place filter systems in major

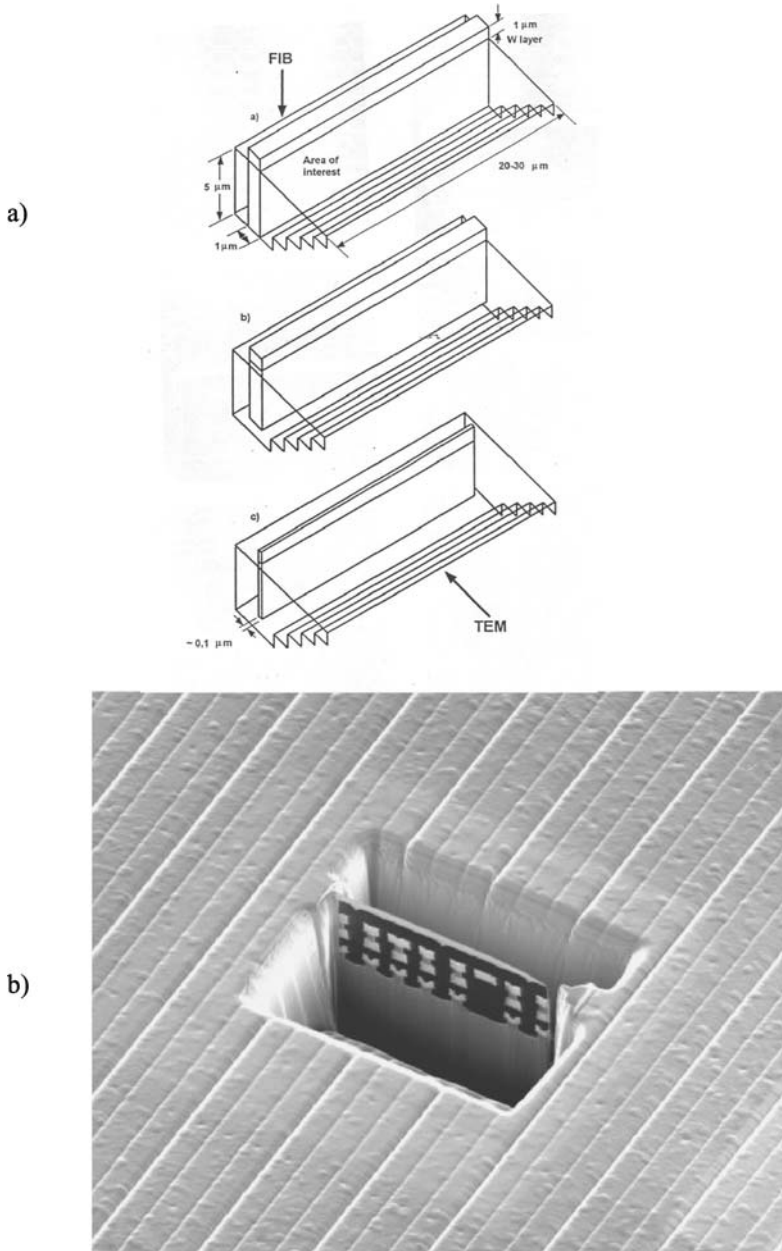


**Figure 25.** (a) Schematic of FIB cutting for TEM sample prep [39]. (b) SE image of sample directly before actual lift out. (Courtesy of FEI Company)



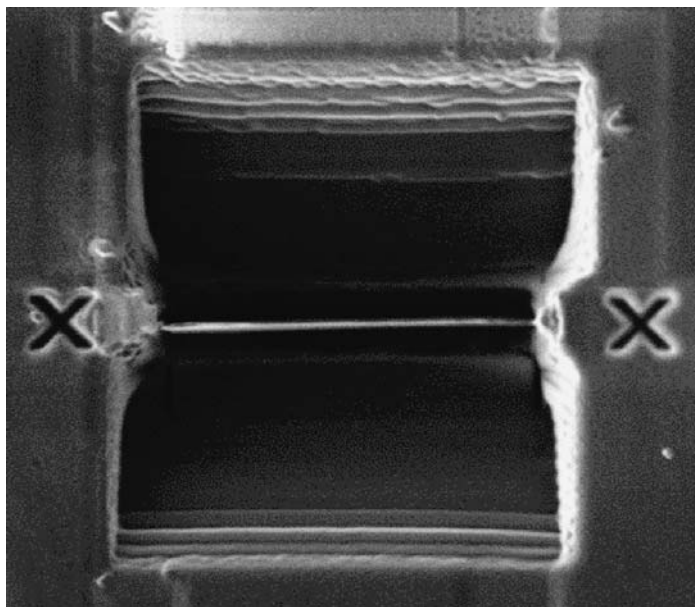


**Figure 26.** Image of warping effect. Cuts will be made around two endpoints to decrease warping.

runoff areas, the focus of a study done by the Swiss Federal Institute for Environmental Study and Technology. Iron hydroxide was found to be the most effective Cu filter. Testing focused on Cu adsorption on suspended specimens in the water as well in the iron hydroxide. TEM was used with iron hydroxide samples prepared using the FIB lift out technique, and it was found that indeed the iron hydroxide was effective in decreasing the copper runoff [43].

With TEM sample preparation, as with most other FIB applications, the two-beam system can provide certain advantages beyond those already discussed. Sivel *et al.* have studied two cases in which the two-beam FIB system has succeeded where other methods have failed. In the first, the two-beam was used to make samples for TEM imaging of an interface in a metal/organic coating sample (figure 27). The samples were composed of an 80  $\mu\text{m}$  thick epoxy coating applied onto a 1 mm thick aluminum alloy. Sample preparation of interfaces is generally difficult because of the different mechanical properties of the two layers, but while conventional ion milling damaged the sample, preparation using the two-beam was successful. Similarly, the two-beam was needed to successfully prepare a TEM sample of a grain boundary in a  $\text{Cu}_3\text{Au}$  alloy [44].

The TEM itself has a wide-range of uses, which can all now be added to the list of applications for which the FIB system is helpful. Undoubtedly, using the FIB has made improvements in both speed and quality of TEM sample production, and is a most important tool to have available.

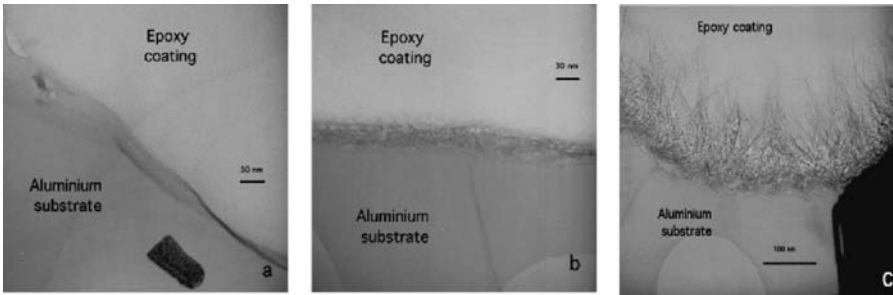


**Figure 27.** (a) Bright-field TEM image of the aluminum-epoxy interface of sample 1. No interface layer is visible. (b) TEM image of sample 2. A regular 30-nm-thick hydroxide layer is visible at the interface. (c) TEM image of the interface of sample 3. A 150-nm-thick pseudoboehmite layer can be seen. The epoxy coating has fully penetrated the rough pseudoboehmite layer [44].

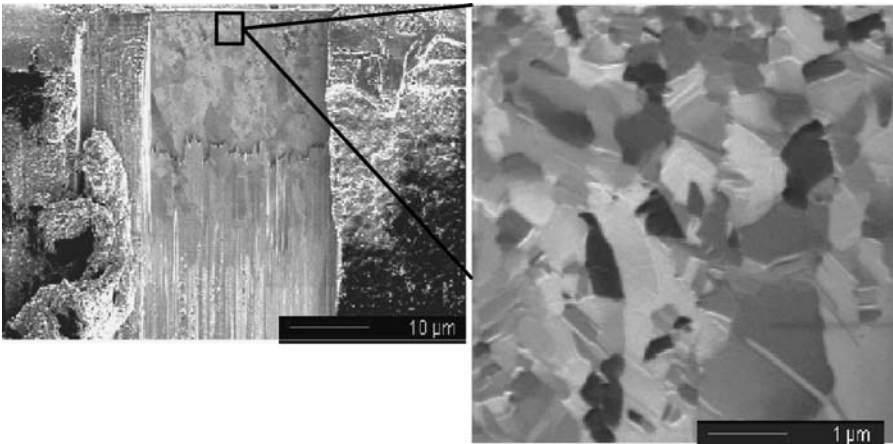


**Figure 28.** High grain boundary definition in Nickel Polycrystals ion beam image [45].

### 3.3. Sample Imaging—Defining the Third Dimension

As discussed earlier, the FIB machine has the capability to image a surface, and the two-beam system in particular can obtain images using either an electron beam or an ion beam. Using the ion beam is advantageous for obtaining images that illustrate high grain boundary definition, as compared to the electron beam which gives crisp resolute surface images. This feature of ion beam images can be observed in work done on modeling the plasticity in LIGA nickel MEMS structures (figure 28) [45]. Though there have been marked advancements in FIB imaging such as adding oxides or carbides for enhancement, one must be aware that using the focused ion beam to image a surface will damage the surface to some extent. This is where the advantages

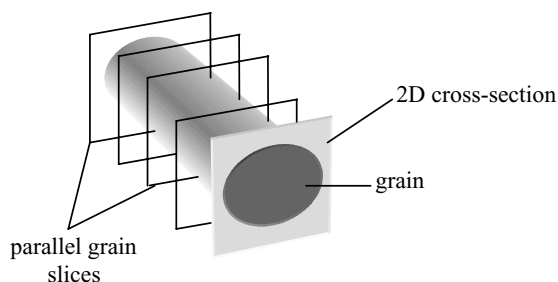


**Figure 29.** Schematic of cross sectioning for grain shape determination.

of the two-beam system come into play by allowing the user to switch back and forth between etching with the FIB and imaging with the SEM [7, 18, 46].

What is so unique about the FIB machine is its ability to uncover the third dimension of a material for imaging. Revealing the internal structure is of the utmost importance to many researchers because it yields valuable information regarding the properties of the material and predictable behavior under certain conditions. In particular, studying the grain structure or grain boundary of a material can provide good insight. In this respect, the two-beam FIB machine can be of great aid. Three-dimensional images are put together using a group of two dimensional images, obtained by shearing off sections of a sample using the FIB, then imaging with the SEM (figure 29). Interpolation of the graphs gives a three-dimensional representation, and important data about the grain structure and other features can then be attained. Internal elemental distribution can also be obtained using SIMS [18, 46]. Dunn and Hull recently demonstrated this ability of the FIB to create three-dimensional volume reconstructions. Their method used FIB serial sectioning and linear interpolation, and was able to produce well defined images of the sample's 3d structure (figure 30) [47].

Cross-sectioning with data analysis using the FIB machine has also been shown to be useful in investigating the effect of additive exposure. A study done at the University of Tokyo used the FIB machine to create cross sections in non-woven fibers with additives for spatial and distribution analysis. Researchers took non-woven polyester fiber samples and added Chimassorb 944, an additive known to improve the functionality of the fiber. Elemental distribution was of particular interest, and a new method of gathering this data was performed using FIB/SIMS technology. Samples of altered fiber were cross sectioned throughout the interior and surface in 3 different manners: perpendicular to the fibers, at a  $45^\circ$  angle, and parallel to the length of the fibers. SIMS mapping was then performed on the cross sections yielding the desired chemical distribution. Signals for  $C^-$ ,  $O_2^-$ ,  $AlO^-$ ,  $Na^+$ ,  $K^+$ ,  $Ca^+$ ,  $CaO^+$ , and  $C^+$  ions were detected, analyzed and mapped for three-dimensional spatial analysis. Voids were found in the material where the additive seemed to concentrate, but most importantly a method of three-dimensional analysis using FIB/SIMS/SEM technology was proven successful (figure 31) [48].

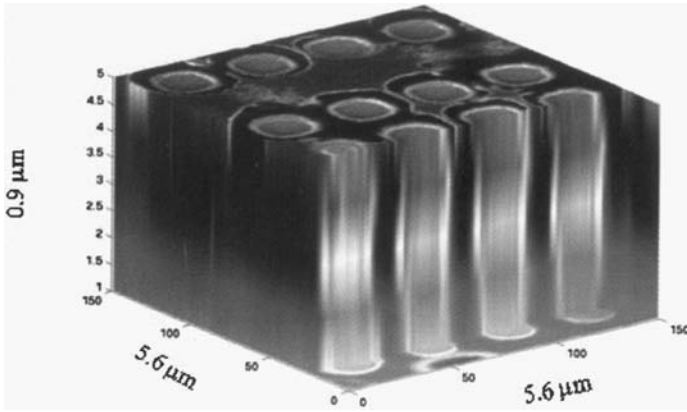


**Figure 30.** An array of vias reconstructed from a series of secondary electron images collected as a function of depth [47]

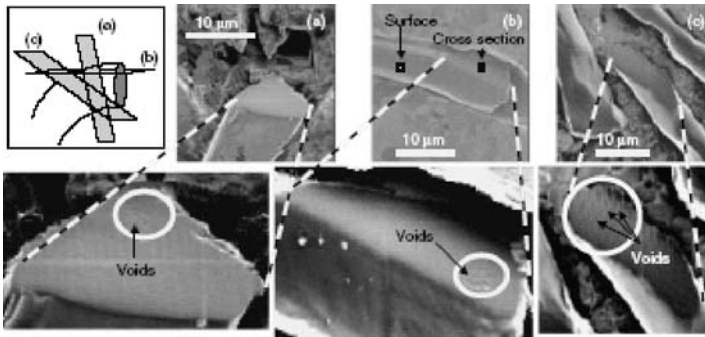


**Figure 31.** Focused Ion beam-induced secondary electron images. The cross-section is approximately perpendicular (a), parallel (b) and  $45^\circ$ . (c) to the longitudinal of the fiber, respectively, as shown in the diagram [48].

As usual, these are just a minute sample of the ways the FIB has been applied to 3D imaging purposes. Nonetheless, they demonstrate the great success and practicality of the FIB system, characteristics that make it an ideal tool.

### 3.4. Damage to the Sample Induced by the FIB

Having discussed many of the advantages of using the FIB system, this review would not be complete without a warning of the possibility of causing damage to the sample. Typically, the focused ion beam has several detrimental effects which result from its use. Firstly, bombardment with  $\text{Ga}^+$  ions will likely result in some level of gallium

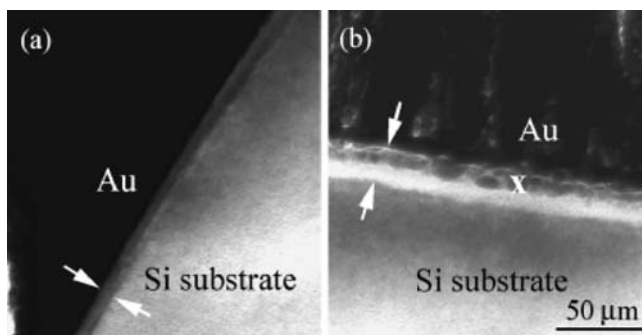


**Figure 32.** The structure of (a) the side-wall and (b) bottom-wall of the trench milled using a 10 keV beam energy and a 250 pA ion beam current [49].

implantation into the surface layers of the sample. Additionally, this bombardment can cause the formation of an amorphous layer, as atoms are knocked out of place and vacancies are created. Finally, some heterogeneity in thickness can occur by means of preferential sputtering or redeposition. It is very important that we gain an understanding of the nature and cause of this sample damage, so that we are both able to recognize it and develop techniques to minimize its occurrence.

Many studies of FIB-induced damage have been undertaken. For example, Rubanov *et al.* looked at cross-sections of trenches milled using the FIB to observe the types and range of damage incurred. They discovered that side-wall damage layers were amorphous, a direct result of using the gallium beam. As for the bottom-wall damage, the group found that there was a layer of material rich in gallium, and that local recrystallization had occurred (figure 32). They experimented with different beam energies, and noted that a reduction from 30 keV to 10 keV cut the thickness of the damage layer in half. In more complex milling patterns, redeposition often occurred [49].

Of course, these limitations of the FIB should not discourage the use of the FIB machine for research. It is the very ability to cause damage to the sample that gives the FIB its remarkable range of capabilities and applications. In addition, several methods to reduce the damaging effect are being developed, each of which has both benefits and weaknesses. Sutton *et al.* looked at the affect of the sample tilt, and noted that the depth of damage could be decreased by tilting the specimen by angles between 4 and 8 degrees at the end of the thinning process. The downside of this technique is its inability to create parallel sidewalls for chemical analysis [50]. Alternatively, using the GAE techniques discussed earlier has been shown to not only increase the etching rate, but also reduce the rate of re-deposition and gallium implantation [51]. The optimal method depends on the needs of the specific user and experiment, but in almost all cases, the FIB is considered as a versatile tool that combines both nanofabrication and microscopy capabilities for nanotechnology research.

## ACKNOWLEDGEMENTS

The author is grateful to his students: Nathan Etessami, Gabriel Mas, Fei Wang, who have partially contributed in preparation of the manuscript; to the National Science Foundation-MRSEC program and New Jersey Commission of Science and Technology for their support.

## REFERENCES

1. Krohn, V. E. *Progr. Astronautics R* (1961) 73.
2. Krohn, V. E. and Ringo, G. R., "Ion source of high brightness using liquid metal", *Appl. Phys. Lett.* **27** (1975) 479.
3. Orloff, J., Utlaut, M., and Swanson, L., *High Resolution Focused Ion Beams: FIB and Its Applications*, Kluwer Academic/Plenum Publishers, New York, NY (2003).
4. Phaneuf, M.W., Applications of focused ion beam microscopy to materials science specimens, *Micron*, **30** (1999) 277.
5. Van Doorselaer, K., Van den Reeck, M., Van den Bempt, L., Young, R., and Whitney, J., How to Prepare Golden Devices Using Lesser Materials in, *Proc. 19th International Symposium for Testing and Failure Analysis* (1993).
6. Russell, P. E., Stark, T. J., Griffis, D. P., and Gonzales, J. C., Chemically Assisted Focused Ion Beam Micromachining: Overview, Recent Developments and Current Needs, *Microsc. Microanal.*, **7S2** (2001) 928.
7. Phaneuf, M. W. and Li, J., FIB Techniques for Analysis of Metallurgical Specimens, *Microsc. Microanal.*, **6S2** (2000) 524.
8. Gerlach, R. and Utlaut, M., Focused ion beam methods of nanofabrication: room at the bottom, *Proc. SPIE Int. Soc. Opt. Eng.*, **4510** (2001) 96.
9. Mitsuishi, K., Shimojo, M., Han, M., and Furuya, K., Electron-beam-induced deposition using a subnanometer-sized probe of high-energy electrons, *Appl. Phys. Lett.*, **83** (2003) 2064.
10. Khizroev, S., Bain, J. A., and Litvinov, D., Fabrication of nanomagnetic probes via focused ion beam etching and deposition, *Nanotechnology*, **13** (2002) 619.
11. Allameh, S. M., Yao, N., and Soboyejo, W. O., Synthesis of self-assembled nanoscale structures by focused ion-beam induced deposition, *Scripta Mater.*, **50** (2004) 915.
12. Strobel, M., Heinig, K.-H., and Möller, W., Can core/shell nanocrystals be formed by sequential ion implantation? Predictions from kinetic lattice Monte Carlo simulations, *Nucl. Instr. Meth. B*, **148** (1999) 104.
13. Young, R. J., Application of the focused ion beam in materials characterization and failure analysis, *Microstructural Science*, **25** (1997) 20.
14. Bender, H., Voltage contrast in the focused ion beam, *Scope*, **13** (2001).
15. Shih, W. C., Ghiti, A., Low, K. S., Greer, A. L., O'Neill, A. G., and Walker, J. F., Analysis of Geometrical and Microstructural Effects on Void Formation in Metallization: Observation and Modeling, *Mater. Res. Soc. Symp. Proc.*, **428** (1996) 243.
16. Crow, G. A., Christman, L., and Utlaut, M., A focused ion beam secondary ion mass spectroscopy system, *J. Vac. Sci. Technol. B*, **13** (1995) 2607.
17. Dong, L. F., Jiao, J., Tuggle, D. W., and Foxley, S., Synthesis and Characterization of Carbon Nanotubes on Porous Silicon Substrates, *Microsc. Microanal.*, **7S2** (2001) 398.
18. Hull, R., Dunn, D., and Kubis, A., Nanoscale Tomographic Imaging Using Focused Ion Beam Sputtering, Secondary Electron Imaging and Secondary Ion Mass Spectrometry, *Microsc. Microanal.*, **7S2** (2001) 34.
19. Gnauck, P., Zeile, U., Rau, W., and Schumann, M., Real time SEM imaging of FIB milling processes for extended accuracy in Cross Sectioning and TEM Preparation, *Microsc. Microanal.*, **9S3** (2003) 524.
20. Zimmermann, G. and Chapman, R., In-Situ Dual Beam (FIBSEM) Techniques for Probe Pad Deposition and Dielectric Integrity Inspection on 0.2 mm Technology DRAM Single Cells in, *Proc. 25th International Symposium for Testing and Failure Analysis* (1999).

21. Lipp, S., Frey, L., Lehrer, C., Frank, B., Demm, E., Pauthner, S., and Ryssel, H., Tetramethoxysilane as a precursor for focused ion beam and electron beam assisted insulator (SiO<sub>x</sub>) deposition, *J. Vac. Sci. Technol. B*, **14** (1996) 3920.
22. Rice, L., Semiconductor Failure Analysis Using EBIC and XFIB, *Microsc. Microanal.*, **7S2** (2001) 514.
23. Huey, B. D. and Langford, R. M., Low-dose focused ion beam nanofabrication and characterization by atomic force microscopy, *Nanotechnology*, **14** (2003) 409.
24. Walker, J. F., TEM sample preparation: site specific search strategy, FEI Europe Ltd.
25. Haythornthwaite, R., Nxumalo, J., and Phaneuf, MW., Use of the focused ion beam to locate failure sites within electrically erasable read only memory microcircuits, *J. Vac. Sci. Technol. A*, **22** (2004) 902.
26. Li, H. W., Kang, D. J., Blamire, M. G., and Huck, W. T. S., Focused ion beam fabrication of silicon print masters, *Nanotechnology*, **14** (2003) 220.
27. Liu, Y., Longo, D. M., and Hull, R., Ultrarapid nanostructuring of poly(methylmethacrylate) films using Ga<sup>+</sup>, *Appl. Phys. Lett.*, **82** (2003) 346.
28. Arshak, K., Mihov, M., Arshak, A., McDonagh, D., and Sutton, D., Novel dry-developed focused ion beam lithography scheme for nanostructure, *Microelectron. Eng.*, **73–73** (2004) 144.
29. Harris, G. and Zhou, P., The Growth and Characterization Processes of Gallium Nitride (GaN) Nanowires, *National Nanofabrication User Network*, **2001** (2001) 34.
30. Flierl, C., White, I. H., Kuball, M., Heard, P. J., Allen, G. C., Marinelli, C., Rorison, J. M., Penty, R. V., Chen, Y., and Wang, S. Y., Focused ion beam etching of GaN, *MRS Internet J. N. S. R.*, **4S1** (1999) G6. 75.
31. Bischoff, L., Teichert, J., Kitova, S., and Tsvetkova, T., Optical pattern formation in a-SiC : H films by Ga<sup>+</sup> ion implantation, *Vacuum*, **69** (2002) 73.
32. Anzalone, P. A., Mansfield, J. F., and Giannuzzi, L. A., DualBeam Milling and Deposition of Complex Structures Using Bitmap Files and Digital Patterning, *Microsc. Microanal.*, **10S2**(2004) 1154.
33. Kang, K. J., Yao, N., He, M. Y., and Evans, A. G., A Method for *in-situ* Measurement of the Residual Stress in Thin Films by Using the Focused Ion Beam, *Thin Solid Films*, **443** (2003) 71.
34. Yao, N., Evans, A. G., and Cooper, C. V., Wear mechanisms operating in diamond like carbon coatings in contact with machined steel surfaces, *Surface and Coatings Technology*, **179** (2004) 306.
35. Chen, X., Wang, R., Yao, N., Evans, A. G., Hutchinson, J. W., and Bruce, R. W., Foreign Object Damage in a Thermal Barrier System: Mechanisms and Simulations, *Materials Science and Engineering A*, **352** (2003) 221.
36. Giannuzzi, L. A., Drown, J. L., Brown, S. R., Irwin, R. B., and Stevie, F. A., Focused ion beam milling and micromanipulation lift-out for site specific cross-section TEM specimen preparation, *Mat. Res. Soc. Symp. Proc.*, **480** (1997) 19.
37. Cairney, J. M., Harris, S. G., Munroe, P. R., and Doyle, E. D., Transmission electron microscopy of TiN and TiAlN thin films using specimens prepared by focused ion beam milling, *Surf. Coatings Technol.*, **183** (2004) 239.
38. Volkert, C. A., Busch, S., Heiland, B., and Dehm, G., Transmission electron microscopy of fluorapatite-gelatin composite particles prepared using focused ion beam milling, *J. Microsc.-Oxford*, **214** (2004) 208.
39. Rossie, B. B., Shofner, T. L., Brown, S. R., Anderson, S. D., Jamison, M. M., and Stevie, F. A., A Method for Thinning FIB Prepared TEM Specimens After Lift-Out, *Microsc. Microanal.*, **7S2** (2001) 940.
40. Yaguchi, T., Konno, M., Kamino, T., Hashimoto, T., Onishi, T., and Umemura, K., FIB Micro-pillar Sampling Technique for 3D Stem Observatin and its Application, *Microsc. Microanal.* 9S2 (2003) 118.
41. Wang, Z. G., Kato, N., Sasaki, K., Hirayama, T., and Saka, H., Electron holographic mapping of two-dimensional doping areas in cross-sectional device specimens prepared by the lift-out technique based on a focused ion beam, *J. Electron Microsc.*, **53** (2004) 115.
42. Walker, J. F., Preparing TEM Sections by FIB: Stress Relief to Straighten Warping Membranes, *Inst. Phys. Conf. Ser.*, **157** (1997) 469.
43. Mavrocordatos, D., Steiner, M., and Boller, M., Analytical electron microscopy and focused ion beam: complementary tool for the imaging of copper sorption onto iron oxide aggregates, *J. Microsc.-Oxford*, **210** (2003) 45.
44. Sivel, V. G. M., Van den Brand, J., Wang, W. R., Mohdadi, H., Tichelaar, F. D., Alkemade, P. F. A., and Zandbergen, H. W., Application of the two-beam FIB/SEM to metals research, *J. Microsc.-Oxford*, **214** (2004) 237.
45. Lou, J., Shrotriya, P., Allameh, S., Yao, N., Buchheit, T., and Soboyejo, W. O., Plasticity Length Scale in LIGA Nickel MEMS Structure, *Mat. Res. Soc. Symp. Proc.*, **687** (2002) 41.

46. Inkson, B. J. and Möbus, G., 3D determination of grain shape in FeAl by focused ion beam (FIB) tomography, *Microsc. Microanal.*, **7S2** (2001) 936.
47. Dunn, D. N., and Hull, R., Three-dimensional volume Reconstructions Using Focused Ion Beam Serial Sectioning, *Microsc. Today*, **12(4)** (2004) 52.
48. Takanashi, K., Shibata, K., Sakamoto, T., Owari, M., and Nihei, Y., Analysis of non-woven fabric fibre using an ion and electron multibeam microanalyser, *Surf. Interface Anal.*, **35** (2003) 437.
49. Rubanov, S. and Munroe, P. R., FIB-induced damage in silicon, *J. Microsc.-Oxford*, **214** (2004) 213.
50. Sutton, D., Parle, S. M., and Newcomb, S. B., Focused ion beam damage: its characterisation and minimization, *Inst. Phys. Conf. Ser.*, **168** (2001) 377.
51. Russell, P. E., Stark, T. J., Griffis, D. P., Phillips, J. R., and Jarausch, K. F., Chemically and geometrically enhanced focused ion beam micromachining, *J. Vac. Sci. Technol. B*, **16** (1998) 2494.